

## Chapter 5 Surface and bulk passivation of GaAs grown on Si substrate by $H_2+PH_3$ plasma and its application for solar cells

### 5. 1 Introduction

Usually, dislocation in GaAs/Si solar cells degrades both short-circuit current density ( $J_{sc}$ ) and open-circuit voltage ( $V_{oc}$ ), especially the  $V_{oc}$ .<sup>1)</sup> It suggests that the key to improving the efficiency of GaAs/Si solar cells lies in increasing the open-circuit voltage. Pearton et al. reported that hydrogen (H) atoms incorporation is an effective way to passivate the electrical activity of defects and impurity states in GaAs/Si epilayer.<sup>2)</sup> As described in previous chapters, there has recently been a renewed interest in the development of hydrogen (H) plasma passivation method for GaAs/Si , which have lead to improved optical and electrical properties. In addition, as described in chapter 3, we have succeeded in increasing the conversion efficiency of GaAs/Si solar cells through hydrogen plasma exposure.<sup>3)</sup> But due to the high reactivity of atomic hydrogen with the surface of III-V compounds, exposure to H plasma also induces etching and damage in the near surface region.<sup>4)</sup> It is necessary to minimize these negative influence of plasma-induced damages. Phosphidization of the GaAs surface by phosphorus (P) atom incorporation has been extensively investigated.<sup>5)</sup> Via a As/P exchange mechanism, a passivating cover layer of gallium phosphide (GaP) is formed. The GaP top layer protects the GaAs surface from oxidation and reduces the surface state density.<sup>6)</sup> Some improvement in the electrical properties of GaAs Schottky diodes has been reported.<sup>7)</sup> The P atoms are substituted for As-related defect centers and suppress the generation of EL2 centers near the surface. Consequently, the presence of atomic P in the plasma is effective in suppressing the generation of plasma-induced damages. In the present study, MOCVD-grown GaAs/Si epilayers are exposed to  $PH_3/H_2$  ( $PH_3/H_2=10\%$ ) plasma which involves both atomic P and H. In this passivation technique, while passivating the shallow levels and defect-related deep levels in

GaAs/Si by H incorporation, the surface phosphidization are realized.

In this chapter, the passivation effects of  $\text{PH}_3/\text{H}_2$  plasma exposure on the optical and electrical properties of GaAs/Si were characterized by auger electron spectroscopy (AES), x-ray photoelectron spectroscopy (XPS), capacitance-voltage (C-V), photoluminescence (PL) and time-resolved photoluminescence (TRPL). For the GaAs/Si solar cells, a significant increase in open circuit voltage was realized only by  $\text{PH}_3/\text{H}_2$  plasma passivation. As a result, the conversion efficiency was improved. Moreover, the annealing effect on  $\text{PH}_3/\text{H}_2$  plasma passivated GaAs/Si were analyzed. It was found the passivation effects was still stable under the  $450^\circ\text{C}$  annealing in  $\text{H}_2$  ambient, thus very useful for technological process. The organization of this chapter is as follows: In section 5. 2, the experimental procedal are described. The GaAs epilayer and the change induced by  $\text{PH}_3+\text{H}_2$  plasma passivation on physical properties are characterized in chapter 5. 3. The  $\text{PH}_3+\text{H}_2$  plasma passivation and annealing effects on photovoltaic properties of GaAs solar cells grown on Si substrates are characterized in 5. 4. Finally, this chapter is summarized in section 5. 5.

## 5. 2 Experimental Procedure

A 3- $\mu\text{m}$ -thick unintentionally doped GaAs top layer was grown at  $750^\circ\text{C}$  using two-step growth method on (100)  $2^\circ$  off towards the [011] Si substrate using conventional atmospheric pressure metalorganic chemical vapor deposition (MOCVD). An AlGaAs (50 nm)/GaAs double heterostructure (DH) with a thickness of 1  $\mu\text{m}$  was also prepared for the time-resolved photoluminescence (TRP) measurement using. The  $\text{p}^+\text{-n}$  GaAs single-junction solar cells with a 50-nm thick AlGaAs window layer on the top were also fabricated. The detailed growth process and the solar cell structure are the same as described in chapter 3. After the growth, passivation was performed in a quartz tube at a reduced pressure ( $\sim 0.1$  Torr) in the ambient of  $\text{H}_2$  or  $\text{H}_2+\text{PH}_3$  (10%). The plasma was excited by radio-frequency (RF) wave via a copper coil encircling the quartz tube. The samples were heated up to  $250^\circ\text{C}$  during the passivation process. The typical

induced RF plasma power and time were 90 W and 1 hour, respectively. The passivated samples were annealed in  $H_2$  ambient at  $450^\circ C$  for 10 minutes in order to evaluate the stability of H and P atoms in GaAs epilayer on Si. After passivation, AuZn/Au and AuSb/Au electrodes were formed by vacuum evaporation for the  $p^+$ -GaAs contact layer and  $n^+$ -Si substrate, respectively. Finally, anti-reflection films were made of  $MgF_2/ZnS$  double layers. The total area of the GaAs solar cell was  $5 \times 5 \text{ mm}^2$ . Four kinds of GaAs/Si solar cells were fabricated: (i) without plasma and annealing treatment (Cell A); (ii)  $H_2$  plasma exposed (Cell B); (iii)  $PH_3/H_2$  plasma exposed (Cell C); and (iv)  $PH_3/H_2$  plasma exposure followed by annealing in  $H_2$  ambient at  $450^\circ C$  (Cell D). Forward dark current-voltage (I-V) characteristics of the GaAs/Si solar cells were measured at room temperature. The photovoltaic properties of these cells were measured under AM0, 1 sun conditions at  $27^\circ C$  using a solar simulator. The values of the photovoltaic properties discussed are active-area values. Carrier concentration profiles were obtained by electrochemical capacitance voltage measurement using a Polaron model PN4200 system. Auger electron spectroscopy (AES) and x-ray photoelectron spectroscopy (XPS) analysis was used to investigate the composition of both the untreated and plasma treated GaAs surfaces. Photoluminescence (PL) spectra were recorded at 4.2 K using a 514.5 nm Ar-ion laser ( $15.07 \text{ W/cm}^2$ ) as an excitation source, and a GaAs photomultiplier tube (PMT) as a detector. Time-resolved photoluminescence (TRPL) was excited by a semiconductor laser pulse ( $\lambda=655 \text{ nm}$ , duration=50 ps) and the TRPL decay curves were measured using the photon counting method at room temperature.

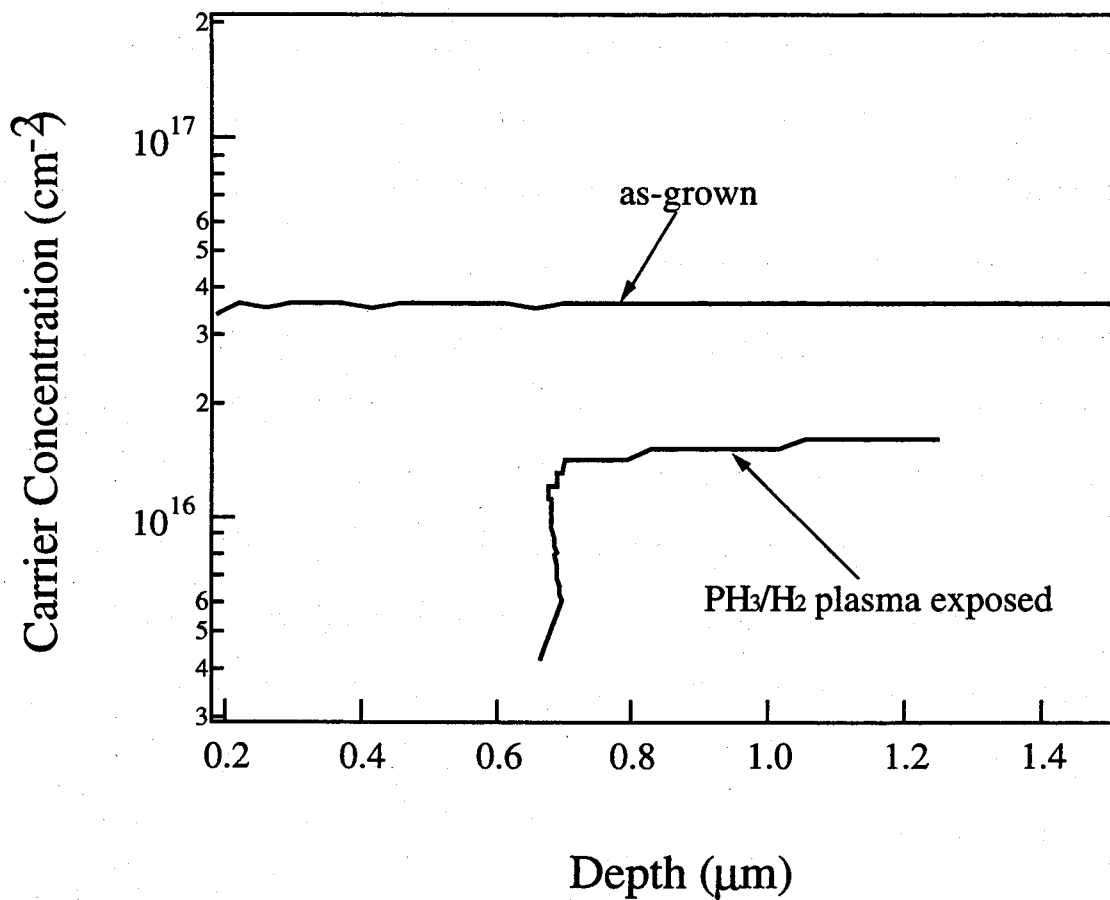


Fig. 5. 1 Free electron concentration depth profiles for as-grown, and PH<sub>3</sub>/H<sub>2</sub> plasma exposed MOCVD-grown unintentionally doped n-GaAs/Si epilayers, respectively.

### 5. 3 Characterization of the passivation effects on GaAs on Si by PH<sub>3</sub>+H<sub>2</sub> plasma exposure

#### 5. 3. 1 Capacitance-voltage profiling study

The MOCVD-grown unintentionally doped GaAs epilayer on Si substrate usually has a high carrier concentration mainly due to the Si auto-doping from the substrate. It was very difficult to grow high resistive undoped GaAs epilayers on Si using the MOCVD technique. The unintentional Si autodoping becomes a crucial problem in the fabrication of GaAs metal-semiconductor field-effect transistors (MESFET's) and high electron mobility transistors (HEMT's), because the pinch-off characteristics of GaAs MESFET's and HEMT's grown on Si by MOCVD are often degraded by unintentional Si autodoping in undoped layers.<sup>8)</sup> The neutralization by H incorporation of the donors Si in GaAs layers has been reported in detail.<sup>9)</sup> It is suggested that the H-Si bonding is response for the neutralization mechanism. As a large number of H atoms are involved in the PH<sub>3</sub>/H<sub>2</sub> plasma, the passivation of Si donors in unintentionally doped GaAs/Si by H atoms is expected.

Figure 5. 1 shows free carrier depth profiles from the unintentionally doped MOCVD-grown GaAs/Si, obtained from electrochemical C-V measurement before and after PH<sub>3</sub>/H<sub>2</sub> plasma exposure. It can be seen that the free carrier concentration decreases dramatically after the passivation process. The carrier concentration of the as-grown sample was  $3.6 \times 10^{16} \text{ cm}^{-3}$ , whereas the PH<sub>3</sub> plasma exposed sample showed a reduced carrier concentration ( $1.5 \times 10^{16} \text{ cm}^{-3}$ ) at the depth of 1  $\mu\text{m}$  from the surface, due to the neutralization of the Si donor by H incorporation. However, the electrical activity of the Si donors was almost restored after annealing at 450°C for 10 min in H<sub>2</sub> ambient. These results were consistent with our previous results of H<sub>2</sub> plasma exposure. These results strongly prove that the PH<sub>3</sub>/H<sub>2</sub> plasma exposure can get the same Si-hydrogenation effects, just as the H<sub>2</sub> plasma exposure.

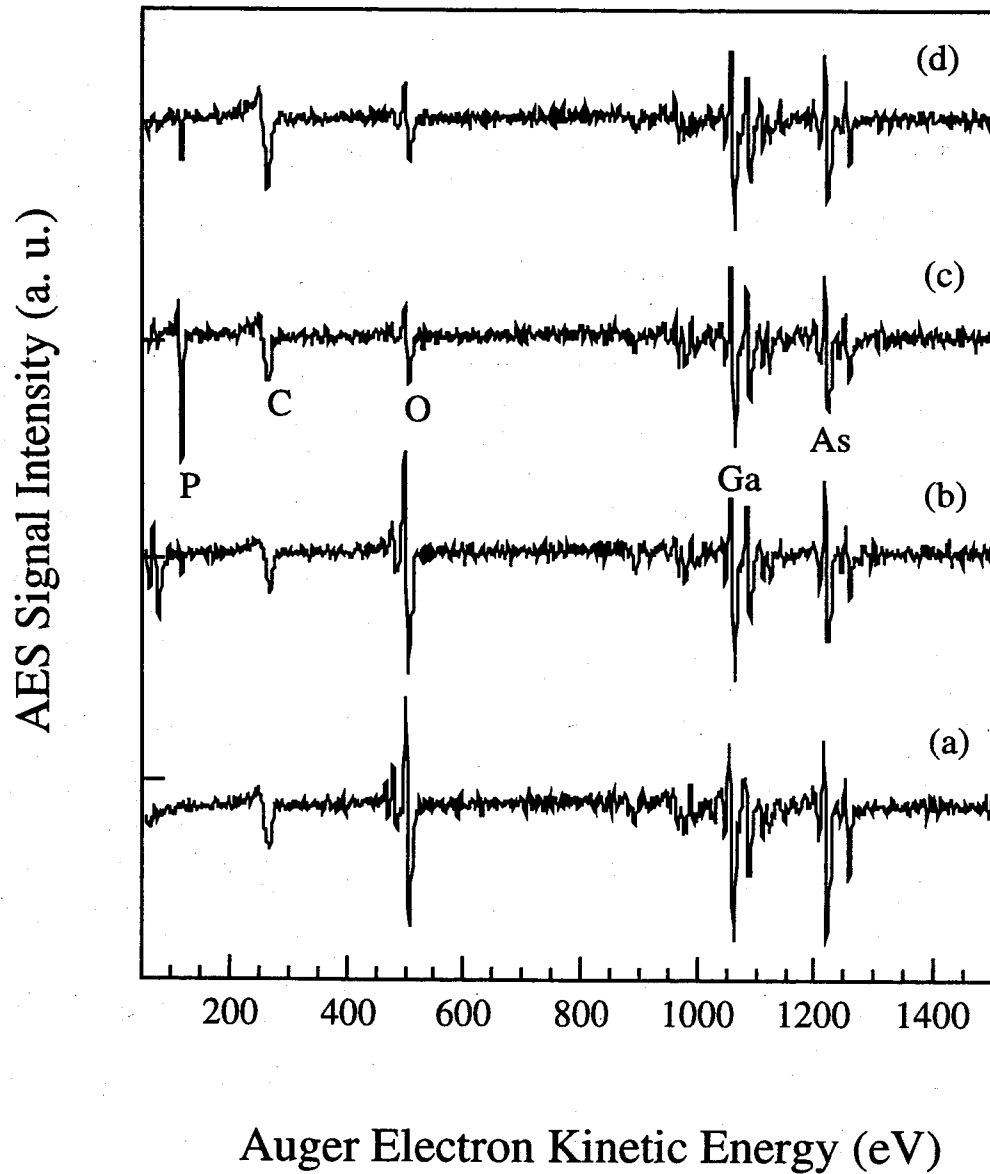


Fig. 5. 2 Auger electron spectra for the surfaces of GaAs epilayers on Si: (a) as-grown, (b) H<sub>2</sub> plasma passivated, (c) PH<sub>3</sub>/H<sub>2</sub> plasma passivated, and (d) PH<sub>3</sub>/H<sub>2</sub> plasma passivated followed by annealing in H<sub>2</sub> ambient at 450°C.

### 5. 3. 2 Auger electron spectroscopy (AES) study

Figure 5. 2 shows the differentiated Auger electron spectrum (AES) of as-deposited and plasma passivated GaAs epilayers grown on Si. Strong O signal originating from oxygen (O) impurity (at ~510 eV) can be observed for the as-deposited sample (spectrum (a) in Fig. 5. 2), and is due to oxidation of the GaAs surface which introduces free arsenic and results in poor surface electronic properties. The H<sub>2</sub> plasma exposure results in a decrease in intensity of the As signal, but no decrease in intensity of the O signal can be observed, as can be seen in spectrum (b) in Fig. 5. 2, suggesting that hydrogen terminated GaAs surface is not efficient in preventing the surface oxidation. The decrease in As may be due to the reaction of H with GaAs, which depletes the As concentration in the surface and induces some As-related deep damages. However, after PH<sub>3</sub>/H<sub>2</sub> plasma exposure, phosphidization of the GaAs surface results in decrease in intensity of the As signal along with a significant decrease in O signal as well as in the appearance of a phosphorus signal at around 119 eV (spectrum (c) in Fig. 5. 2). This can be attributed to replacement of surface As atoms by P atoms, which forms a passivating cover layer of gallium phosphide. Group III-V phosphides are characterized by lower oxidation rate and lower surface state density than the arsenides. Further, P atoms were reported to fill in the plasma-induced As vacancy and suppress the generation of damages.<sup>10)</sup> Annealing the phosphidized sample at 450°C for 10 min in H<sub>2</sub> ambient reduced the intensity of P signal to some extent, but the O signal still remains weak (spectrum (d) in Fig. 5. 2) showing high stability of the surface phosphidization.

The compositional structure was profiled by measuring the Ga-Auger peak (1070 eV), As-Auger peak (1228 eV) and P-Auger peak (119eV) intensities by sputtering. Figure 5. 3 shows the ratios of the Auger signals of As/Ga and P/Ga as a function of sputter time for the GaAs on Si before plasma exposure (A), after PH<sub>3</sub>/H<sub>2</sub> plasma exposure (B) and after annealing at 450°C for 10 minutes in H<sub>2</sub> ambient (C). It was clearly seen that the Auger signal of P atoms was significantly increased whereas that of As atoms was decreased after the PH<sub>3</sub>/H<sub>2</sub> plasma exposure. This furtherly

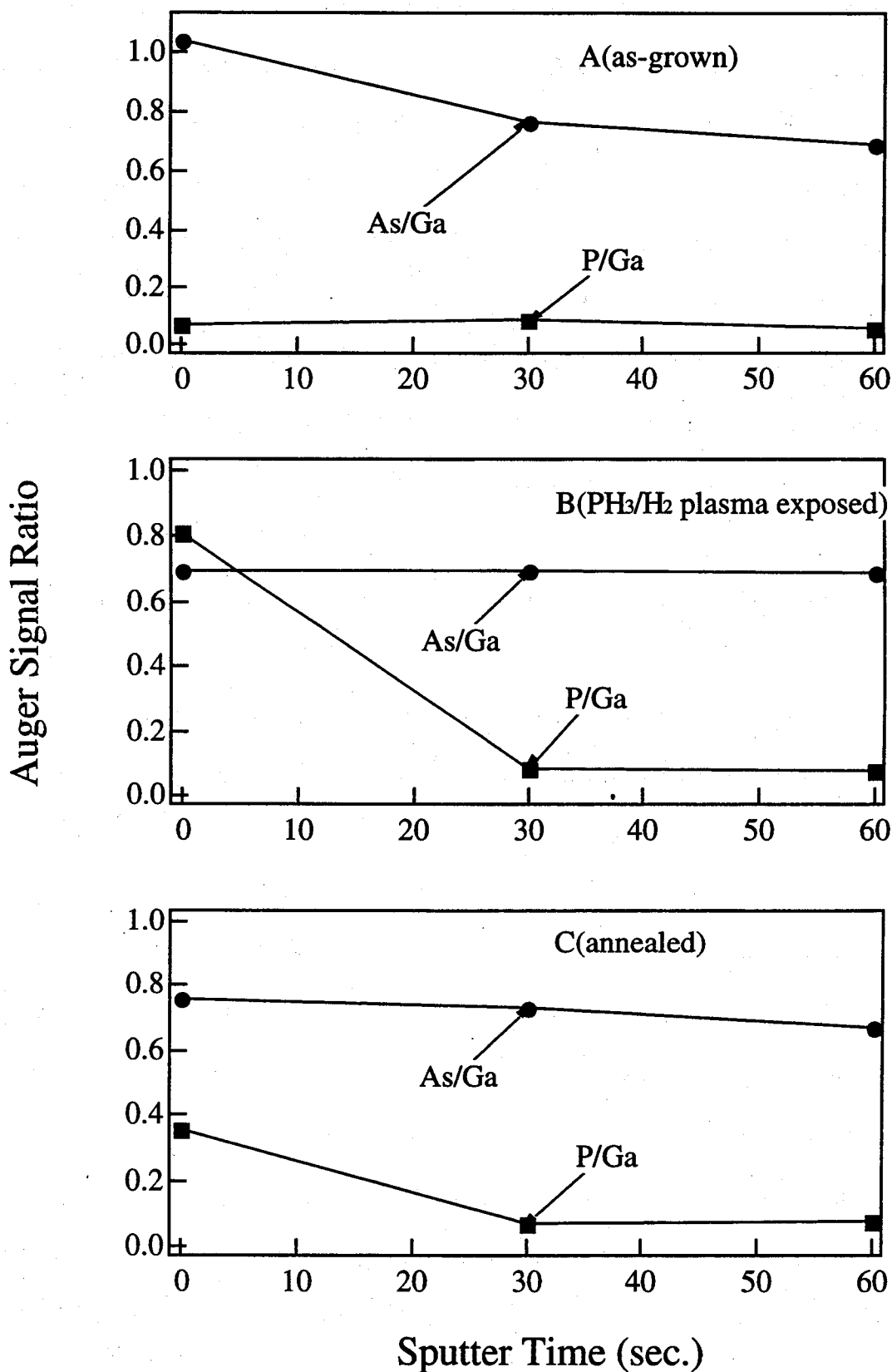


Fig. 5. 3 Auger signals of As/Ga and P/Ga as a function of sputter time for the GaAs/Si epilayers: A. as grown, B. PH<sub>3</sub>/H<sub>2</sub> plasma exposed, C. PH<sub>3</sub>/H<sub>2</sub> plasma exposed then annealed in H<sub>2</sub> ambient at 450°C for 10 min.



confirmed the replacement of surface As atoms by P atoms, which forms a passivating cover layer of gallium phosphide on the surface of GaAs/Si. Group III-V phosphides are characterized by the lower oxidation rate and lower surface states density than the arsenides. However, after removing about 50 Å of the material, which corresponds to 30 sec. sputtering time, the Auger intensity decreased to its reference value. This means that PH<sub>3</sub> plasma exposure only induces a thin superficial P-related layer. That is to say, phosphidization modifies only the GaAs surface or the region located very close to the surface. After annealing the phosphidized sample at 450°C for 10 min in H<sub>2</sub> ambient, the intensity of P signal was still partly remained. This means the surface phosphidization still existed even under this annealing treatment.

### 5. 3. 3 X-ray photoelectron spectroscopy (XPS) study

Figure 5. 4 (a) shows XPS spectra of the Ga 3*d* core level for the as-grown and PH<sub>3</sub>+H<sub>2</sub> plasma exposed GaAs/Si samples. For the as-grown sample, the main signal at the binding energy of 19.5 eV is due to the Ga-As bond. An XPS signal peak at 20.8 eV is also observed in addition to the main peak. This signal is identified as the XPS signal from Ga-related oxide. In the case of the phosphidized GaAs/Si epilayer, the Ga-oxide related peak is apparently diminished, suggesting that the PH<sub>3</sub>+H<sub>2</sub> plasma exposure effectively removed the Ga-related oxide. Fig. 5. 4 (b) shows the XPS spectra of the As 3*d* core for the as-grown and PH<sub>3</sub>+H<sub>2</sub> plasma exposed samples. For the as-grown sample, two signal peaks are observed at the binding energies of 41.5 and 44.9 eV, which are identified with XPS signals due to GaAs and As<sub>2</sub>O<sub>3</sub>, respectively. For the phosphidized sample, only the peak at 41.4 eV is observed, demonstrating that the PH<sub>3</sub>+H<sub>2</sub> plasma exposure effectively removes As oxides. Fig. 5. 4 (c) shows the XPS spectrum from the P 2*p* core level of the PH<sub>3</sub>+H<sub>2</sub> plasma exposed sample. Deconvolution of the broad signal peaked at the binding energy results in two signals at 129.6 and 128.8 eV, which are attributed to P-P and P-Ga bonds<sup>11</sup>. The existence of P-Ga bonds suggests the substitution of P atoms for As atoms. The main peak

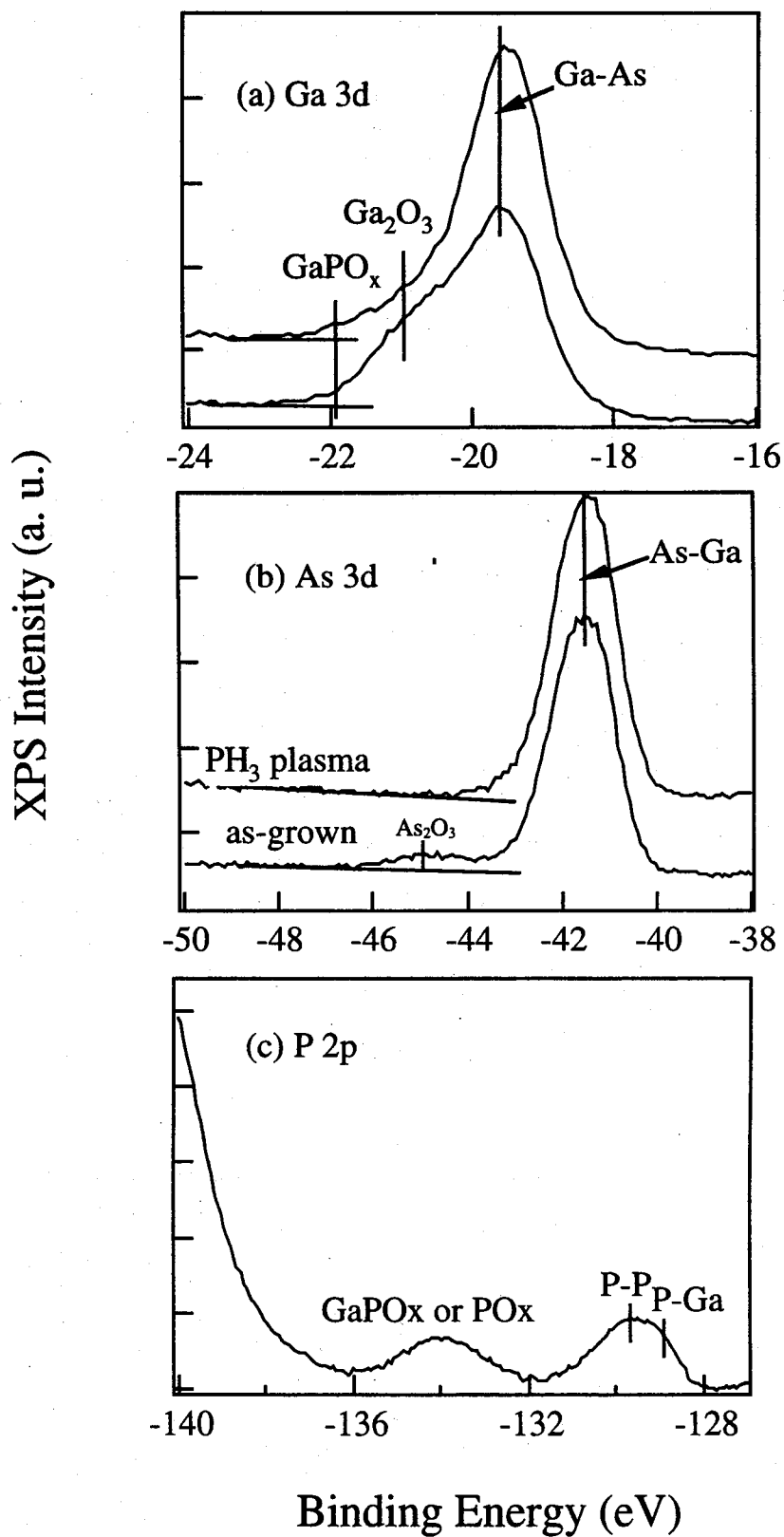


Fig. 5. 4 XPS spectra from Ga 3d, As 3d, and P 2p core levels of as-grown and PH<sub>3</sub>+H<sub>2</sub> plasma exposed GaAs/Si layers.

signal at the binding energy 133.9 eV are identified with XPS signal from  $\text{PO}_x$  and  $\text{GaPO}_x$ , since the phosphidized GaAs/Si surface was exposed to air when the sample is transported from the plasma reactor to the XPS chamber.

### 5. 3. 4 Photoluminescence (PL) study

Figure 5.5 shows 4.2 K PL spectra of the unintentionally doped n-type GaAs ( $3\mu\text{m}$  thick) epilayers on Si substrate. Two dominant peaks appear for the as-grown samples: heavy-hole-associated free-exciton peak A (1.485 eV), and carbon-bound exciton peak B (1.468 eV). Whereas the integrated PL intensity of  $\text{H}_2$  plasma passivated sample, Fig. 5.5 (b), shows almost no increase. PL intensity of  $\text{PH}_3/\text{H}_2$  plasma passivated sample shows a significant increase, as shown in Fig. 5.5 (c), compared to that of the as grown sample, Fig. 5.5 (a). It is attributed to a decrease in surface recombination states caused by surface phosphidization due to  $\text{PH}_3/\text{H}_2$  plasma exposure which protects the surface from oxidation.<sup>12)</sup> However, annealing the  $\text{PH}_3/\text{H}_2$  plasma passivated sample at  $450^\circ\text{C}$  in  $\text{H}_2$  ambient decreases the PL intensity, Fig. 5.5 (d), which suggests that some of the plasma-induced damages are activated at this annealing temperature thereby quenching the PL efficiency.<sup>13)</sup>

Figure 5.6 shows the room-temperature PL spectra measured for GaAs/Si before, and after  $\text{PH}_3/\text{H}_2$  plasma exposure. The room-temperature PL peak was identified as a conduction-band to valence-band transition, since the exciton- and shallow-donor-related luminescence was thermally quenched at room temperature and the band-to-band (BB) recombination dominates the spectra. The room temperature intensity of band-to-band recombination was frequently used to characterize the quantum efficiency of the samples. It can be seen that the  $\text{PH}_3/\text{H}_2$  plasma exposure effectively increased the PL efficiency of the GaAs/Si and decreased the full width at half maximum (FWHM) of the intensity (from 42.4 to 41.1 meV) comparing with that of as-grown sample. As the free carrier concentration of the  $\text{PH}_3/\text{H}_2$  plasma exposed sample was decreased and no increase was

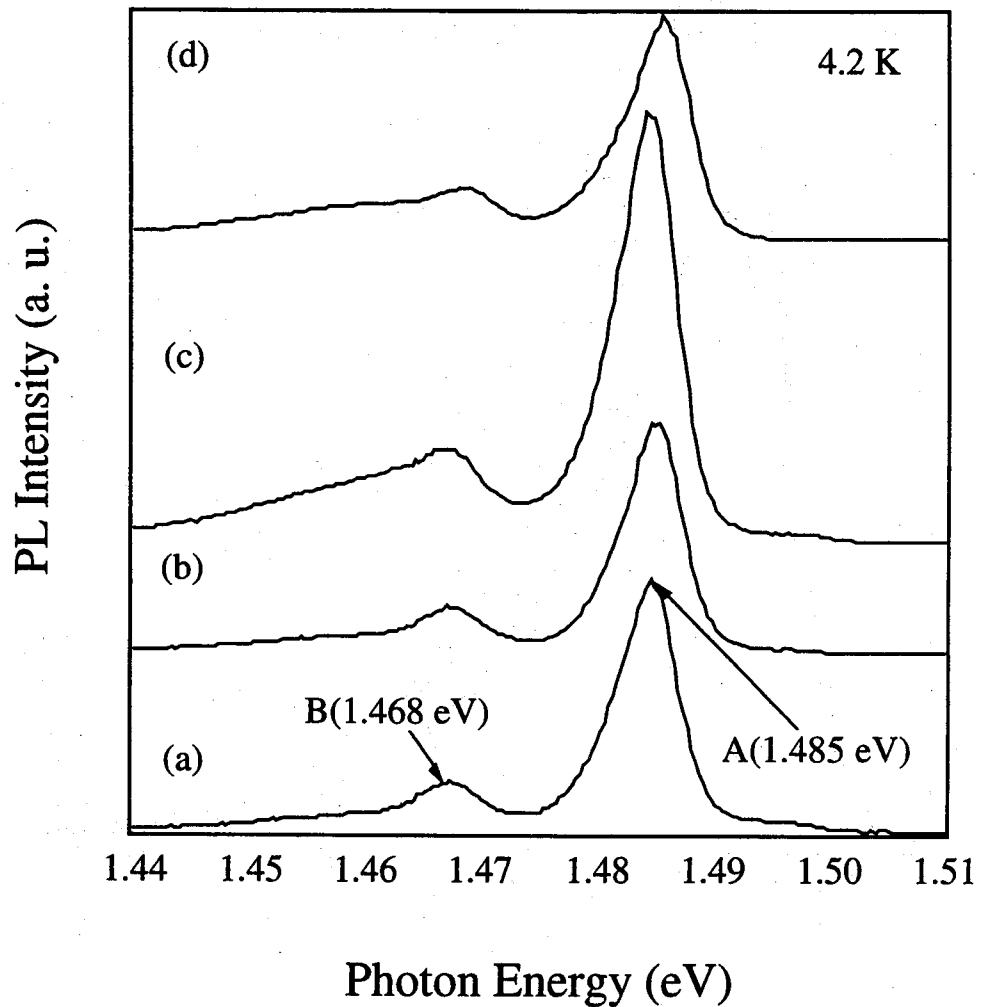


Fig. 5. 5 PL spectra of GaAs epilayers grown on Si substrate recorded at 4.2 K; (a) as-grown, (b) H<sub>2</sub> plasma passivated, (c) PH<sub>3</sub>/H<sub>2</sub> plasma passivated, and (d) PH<sub>3</sub>/H<sub>2</sub> plasma passivated followed by annealing in H<sub>2</sub> ambient at 450oC. Peaks A (1.486 eV) and B (1.468 eV) represent heavy-hole-associated free exciton and carbon-impurity-bound exciton peaks, respectively.

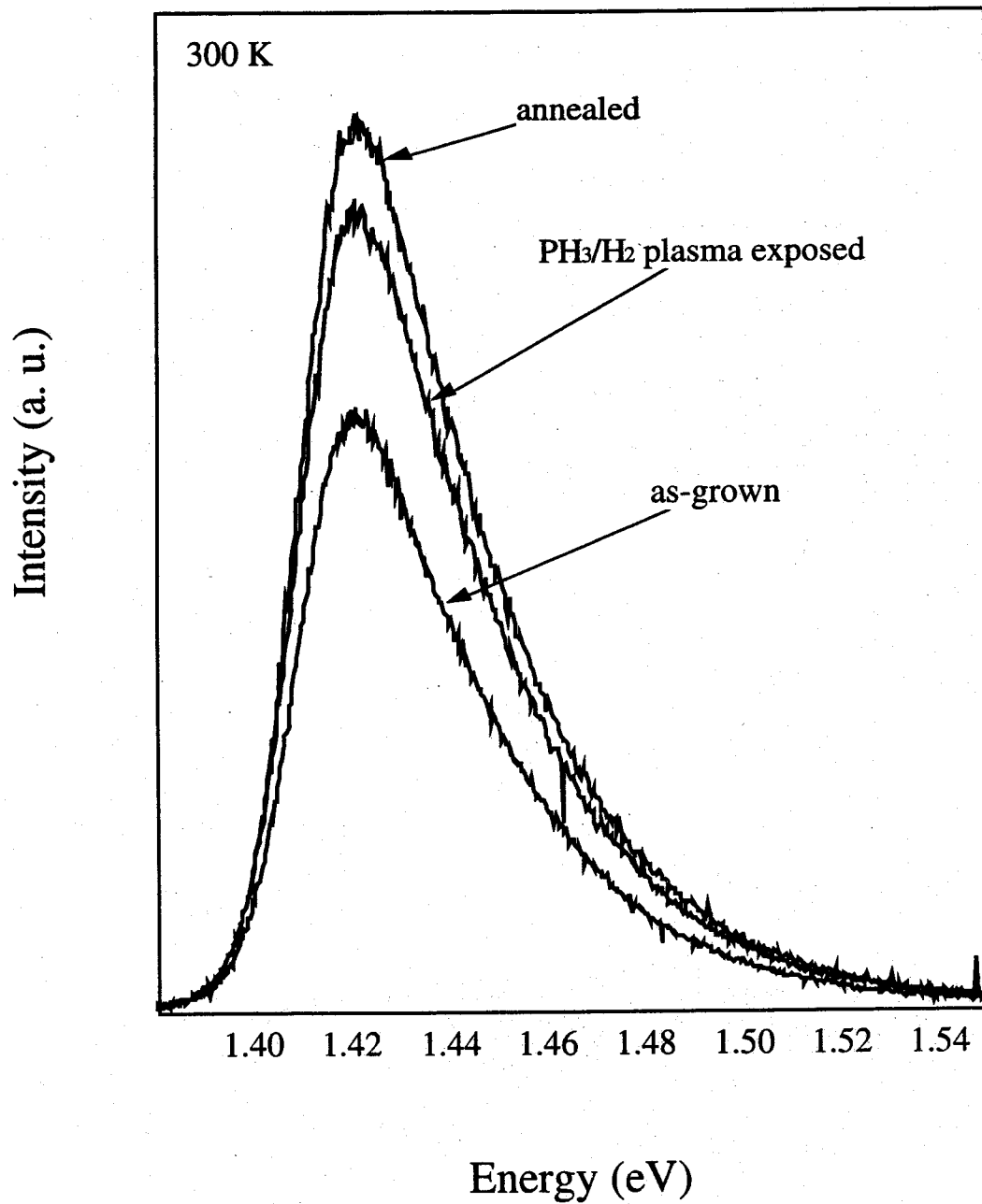


Fig. 5. 6 The room temperature PL spectra of GaAs/Si epilayers for as-grown, PH<sub>3</sub>/H<sub>2</sub> plasma exposed, and PH<sub>3</sub>/H<sub>2</sub> plasma exposed then annealed in H<sub>2</sub> ambient at 450°C for 10 min samples, respectively.

observed for the pure  $H_2$  plasma exposed sample, the enhancement of the room temperature PL intensity can be attributed to the P atoms incorporation into the surface region by  $PH_3/H_2$  plasma exposure, which decrease the surface-state density and lower the surface recombination velocity. After annealing the  $PH_3/H_2$  plasma exposed sample at  $450^\circ C$  for 10 min, the PL intensity was further increased due to the recovery of the electrical activity of the donors (Si) which increased the free carrier concentration. It also suggests that the surface phosphidization effects are thermally stable. However, the plasma passivation effects are not so significant compared with that at 4.2 K. It may be because that the plasma-induced damages in the surface region are not as important in limiting the carrier lifetimes at low temperature as they are at room temperature.

### 5. 3. 5 Time-resolved photoluminescence (TRPL) study

In order to elucidate the passivation effect of nonradiative recombination centers, we also measured the minority carrier lifetime of GaAs on Si using a n-AlGaAs(50nm)/GaAs(2 $\mu$ m) DH structure which is least influenced by the surface condition before and after  $H_2$  or  $H_2+PH_3$  plasma passivation.<sup>14)</sup> The TRPL decay curves are shown in Fig. 5. 7. The improvement of the slope of TRPL decay curve is due to the improvement of the bulk minority carrier lifetime of GaAs epilayer on Si.  $PH_3/H_2$  plasma exposure has been found to increase the minority carrier lifetime more effectively than  $H_2$  plasma exposure. This can only be attributed to the passivation of AlGaAs/GaAs interfacial defects-related nonradiative recombination centers by P atoms incorporation, as the P atoms are found almost concentrated in the surface region ( $\sim 50 \text{ \AA}$ ) by our AES depth profiles measurement. Furthermore, this increase in the minority carrier lifetime still persists to some extent even after annealing at  $450^\circ C$ , and is in good agreement with our previous results where we found that the H passivation effect of some deep defects in GaAs/Si epilayer is stable under  $450^\circ C$  annealing.<sup>14)</sup>

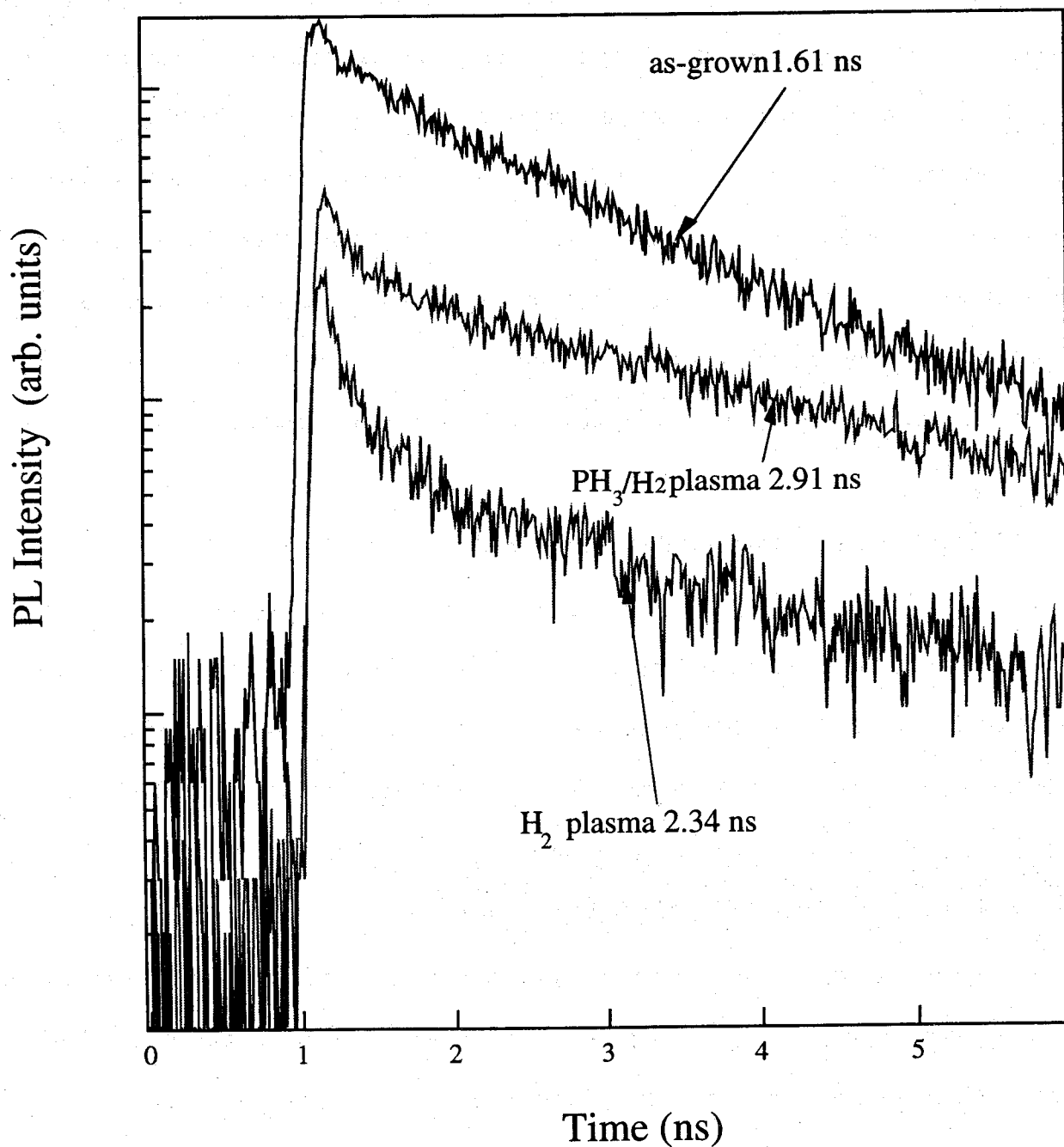


Fig. 5. 7 Time-resolved PL decay curves of AlGaAs/GaAs double hetero structures grown on Si substrates, measured at room temperature for as-grown, H<sub>2</sub> plasma passivated, and PH<sub>3</sub> (PH<sub>3</sub>/H<sub>2</sub>=10%) plasma passivated samples.

#### 5. 4 Characterization of the photovoltaic properties of GaAs on Si solar cells passivated by PH<sub>3</sub>+H<sub>2</sub> plasma

The typical room temperature forward dark current-voltage (I-V) characteristics of GaAs/Si single-junction solar cells are shown in Fig. 5. 8. The saturation current density  $J_0$  of H plasma exposed cell (Cell B) shows a slight decrease from  $1.14 \times 10^{-9}$  to  $7.84 \times 10^{-10}$  A/cm<sup>2</sup> compared to that of the as-grown cell (Cell A), due to the H passivation of electrical activity of the residual defects, such as threading dislocations<sup>15</sup>. For PH<sub>3</sub>/H<sub>2</sub> plasma passivated cell (Cell C), a lowest value of  $5.72 \times 10^{-11}$  A/cm<sup>2</sup> of  $J_0$  is obtained. This further decrease in  $J_0$  by addition of PH<sub>3</sub> to H<sub>2</sub> plasma can only be attributed to the surface phosphidization effects by P atoms incorporation. Annealing the phosphidized cell (Cell D) at 450°C makes it more leaky due to the reactivation of plasma-induced damages, as discussed before. It is very clear that both H and P atoms play an important role in the passivation process by PH<sub>3</sub>/H<sub>2</sub> plasma exposure. In addition, although the H plasma passivation effectively reduces the electrical activity of shallow dopants,<sup>16</sup> the series resistance ( $R_s$ ) of the passivated solar cells is also decreased, which may be due to the passivation of the nonradiative centers in GaAs on Si that increases the mobility.

Figure 5. 9 shows the photovoltaic I-V properties of the above four cells (Cell A, B, C and D) measured under AM0, 1 sun, 27°C conditions. The quantum efficiency of the respective samples are shown in Fig. 5. 10. The results are summarized in Table 5. 1. Compared with the untreated Cell A, the H<sub>2</sub> plasma passivated Cell B shows an increase in both the short-circuit current density,  $J_{sc}$ , from 34.08 to 34.46 mA/cm<sup>2</sup>, and open-circuit,  $V_{oc}$ , from 0.85 to 0.88 V. As a result, the conversion efficiency,  $E_{ff}$ , is increased from 15.9 to 17.6 %. For the PH<sub>3</sub>/H<sub>2</sub> plasma passivated Cell C, very high  $V_{oc}$  (0.93 eV) and FF (80.9%) are obtained due to the very low value of  $J_0$ , leading to further improvement in  $E_{ff}$  (18.6%). However,  $J_{sc}$  of the PH<sub>3</sub>/H<sub>2</sub> passivated cell is also suppressed to some degree, which may be due to the formation of III-V/P compound thin layer over the AlGaAs window layer which causes slightly more photons to be absorbed in the window



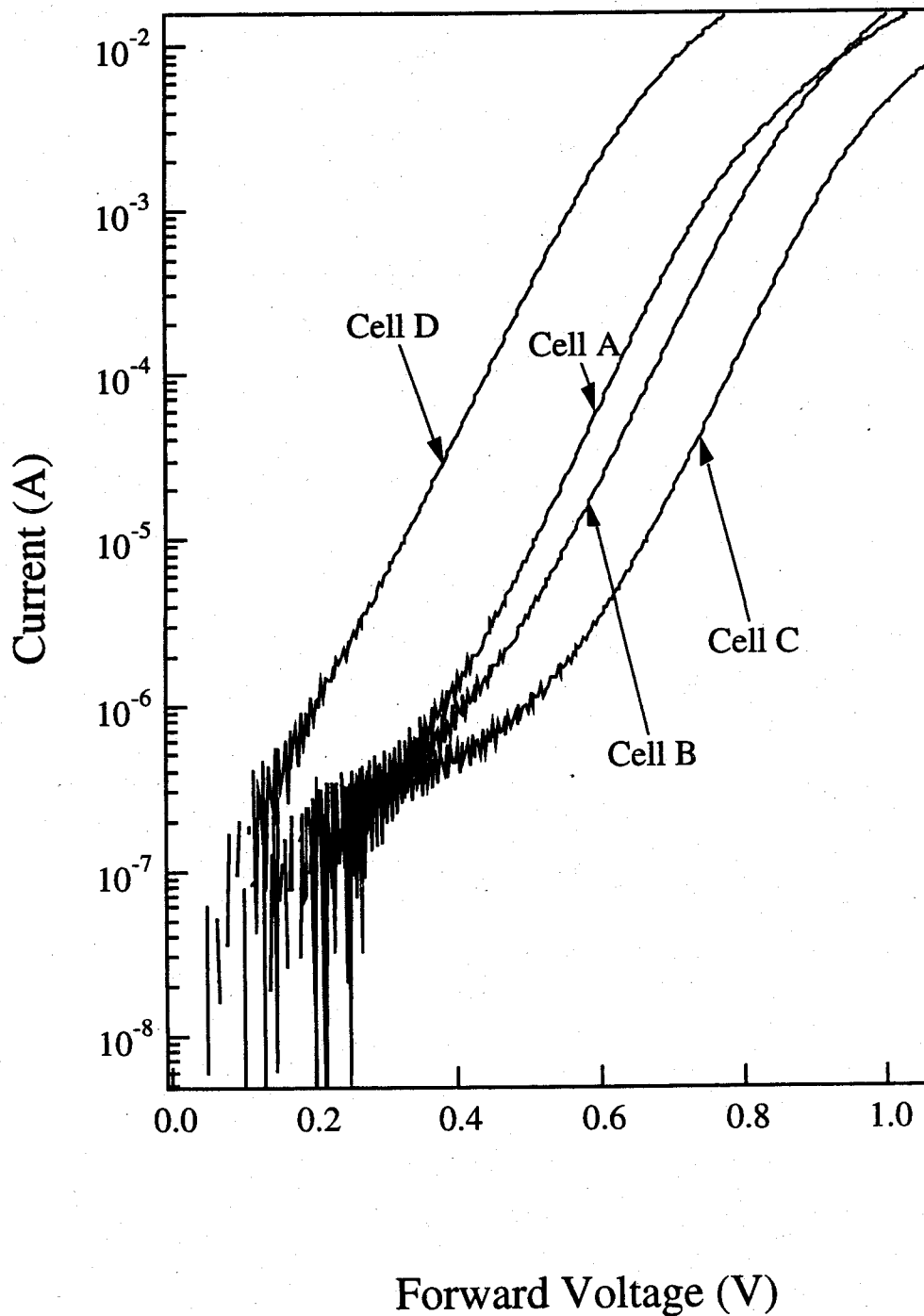


Fig. 5. 8 Forward I-V characteristics of the GaAs/Si p<sup>+</sup>-n junction diodes in dark. Cell A: as-grown ; Cell B: H<sub>2</sub> plasma passivated; Cell C: PH<sub>3</sub>/H<sub>2</sub> plasma passivated, and Cell D: PH<sub>3</sub>/H<sub>2</sub> plasma passivated followed by annealing in H<sub>2</sub> ambient at 450°C. The total junction area is 0.25 cm<sup>2</sup>.

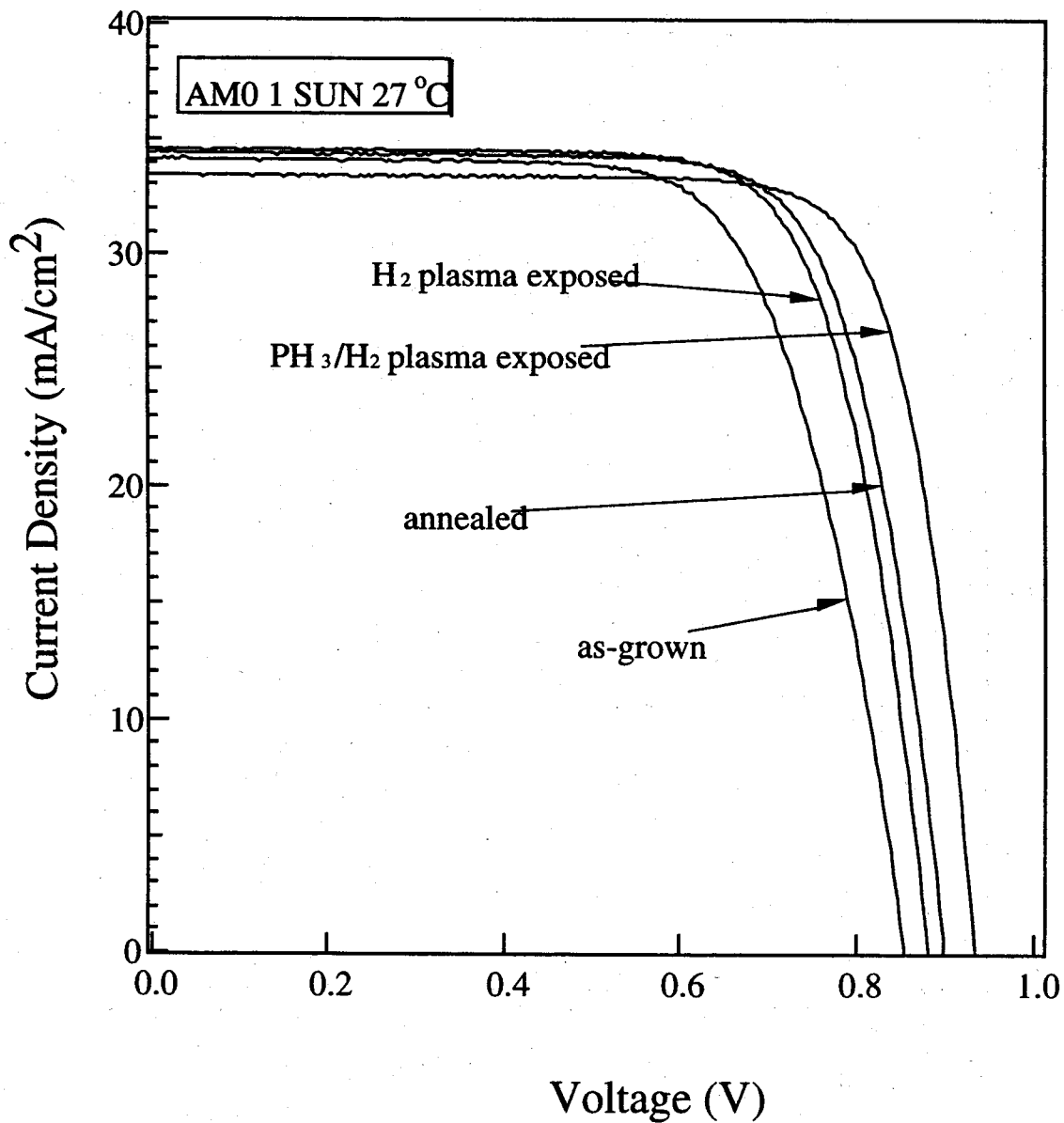


Fig. 5. 9 Current density-voltage characteristics of GaAs/Si single-junction solar cells measured under AM0, 1 sun, 27°C conditions for as-grown, H<sub>2</sub> plasma passivated, PH<sub>3</sub>+H<sub>2</sub> plasma exposed, and PH<sub>3</sub>+H<sub>2</sub> plasma exposed then annealed in H<sub>2</sub> ambient at 450°C for 10 min cells, respectively.

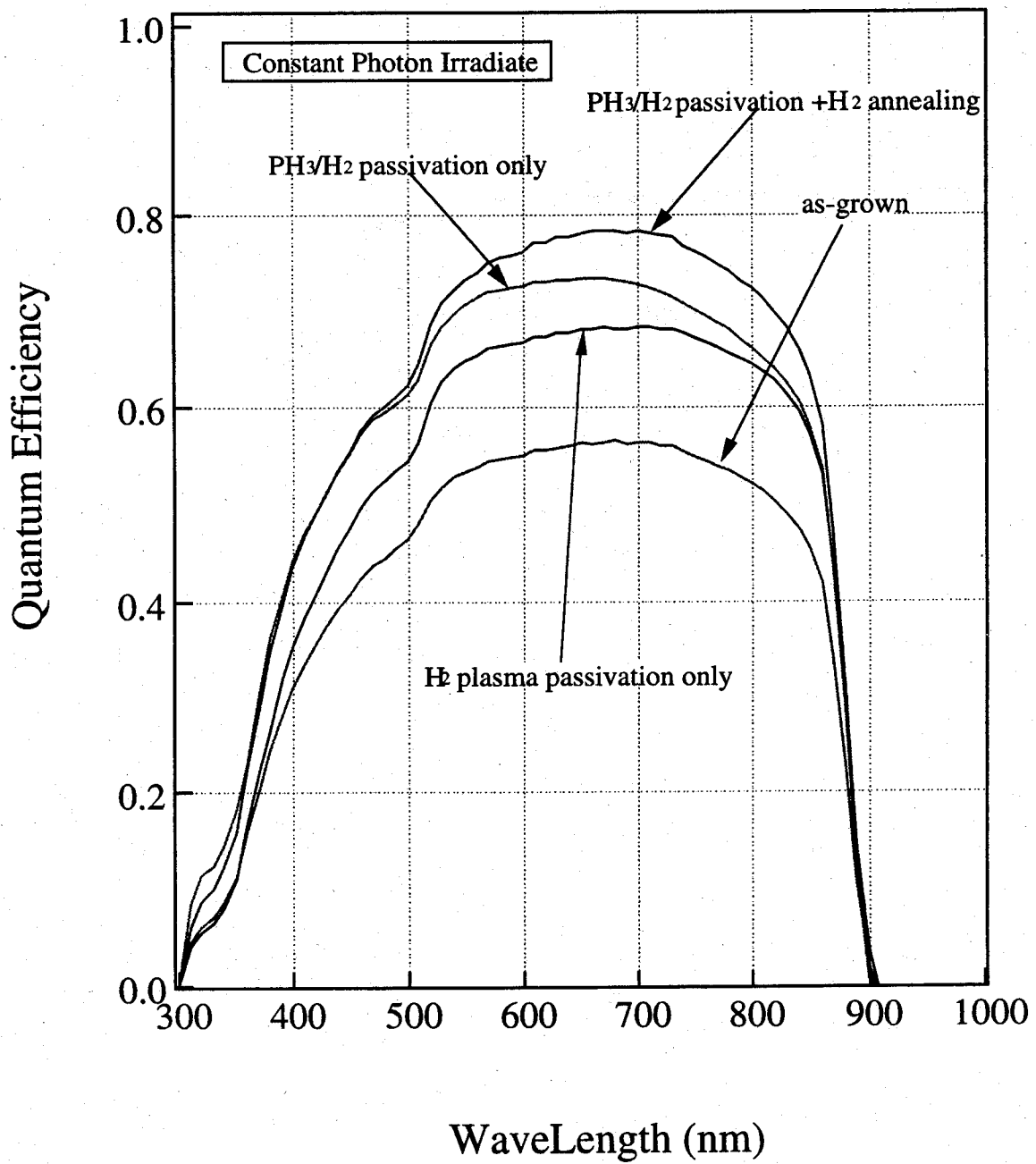


Fig. 5. 10 Quantum efficiencies of GaAs solar cells on Si substrates before and after plasma passivation.

Table 5. 1 The photovoltaic properties of GaAs solar cells on Si under 1 sun AM0 illumination at 27°C. Cell A: as-grown cell, Cell B : passivated by H<sub>2</sub> plasma, Cell C: passivated by PH<sub>3</sub>/H<sub>2</sub> (PH<sub>3</sub>/H<sub>2</sub>=10%) plasma , and Cell D: passivated by PH<sub>3</sub>/H<sub>2</sub> plasma then annealed in H<sub>2</sub> ambient at 450°C.

Sample No.	$J_0$ (A/cm <sup>2</sup> )	$J_{sc}$ (mA/cm <sup>2</sup> )	$V_{oc}$ (V)	FF (%)	$E_{ff}$ (%)
Cell A	$1.14 \times 10^{-9}$	34.08	0.85	73.9	15.9
Cell B	$7.84 \times 10^{-10}$	34.46	0.88	78.6	17.7
Cell C	$5.72 \times 10^{-11}$	33.39	0.93	80.9	18.6
Cell D	$6.00 \times 10^{-8}$	34.32	0.89	78.8	17.9

layer and reduces  $J_{sc}$ .<sup>17)</sup> In order to test the thermal stability, the  $\text{PH}_3/\text{H}_2$  passivated cell was annealed in  $\text{H}_2$  ambient at  $450^\circ\text{C}$ . The annealed cell (Cell D) still showed a very high  $E_{ff}$  (17.9%), suggesting that  $\text{PH}_3/\text{H}_2$  plasma passivation is very useful for practical application, as the process temperature of device fabrication is usually below  $450^\circ\text{C}$ .

## 5. 5 Conclusion

In summary, the  $\text{PH}_3/\text{H}_2$  plasma passivation effects on MOCVD-grown GaAs/Si were studied in detail. It showed that both the surface phosphidization and defect hydrogenation can be realized simultaneously. As a result, the optical and electrical properties of GaAs/Si were effectively improved. Using  $\text{PH}_3/\text{H}_2$  plasma passivation, the surface phosphidization and bulk hydrogenation effects of GaAs/Si solar cells are realized simultaneously. Consequently, the saturation current density of the passivated cell is significantly decreased due to reduction of surface recombination velocity and increase of minority carrier lifetime, resulting in very high  $V_{oc}$  (0.93 V) and FF (80.9) for GaAs/Si solar cell. The  $E_{ff}$  is improved from 15.8 to 18.6% with this single passivation process. Thus  $\text{PH}_3/\text{H}_2$  plasma passivation opens a interesting and promising way to improve the characteristics of GaAs on Si devices.

## References:

- 1) J. C. Zolper and A. M. Barnett, *IEEE Trans. Electron Devices*, **37**, 478 (1990).
- 2) S. J. Pearton, C. S. Wu, M. Stavola, F. Ren, J. Lopata, W. C. Dautremont-Smith, S. M. Wernon and V. E. Haven, *Appl. Phys. Lett.* **51**, 496, (1987).
- 3) G. Wang, K. Otsuka, T. Soga, T. Jimbo and M. Umeno, *Jpn. J. Appl. Phys.* **38**, 3504, (1999).
- 4) P. Friedel and S. Gourrier, *Appl. Phys. Lett.* **42**, 509, (1983).
- 5) T. Sugino, T. Yamada, K. Matsuda and J. Shirafuji, *Jpn. J. Appl. Phys.* **29**, L1575, (1990).
- 6) P. Viktorovitch, M. Gendry, S. K. Krawczyk, F. Krafft, P. Abraham, A. Bekkaoui and Y. Monteil, *Appl. Phys. Lett.* **58**, 2387, (1991).
- 7) T. Sugino, T. Yamada, K. Matsuda and J. Shirafuji, *Appl. Surf. Sci.* **56/58** (1992) 311.
- 8) S. Nozaki, J. J. Murry, A. T. Wu, T. George, E. R. Weber and M. Umeno, *Appl. Phys. Lett.* **55** (1989) 1674.
- 9) S. J. Pearton, W. C. Dautremont-Smith, J. Chevallier, C. W. Tu and K. D. Cummings, *J. Appl. Phys.* **59** (1986) 2821.
- 10) B. I. Bednyi and N. V. Baidus, *Semiconductors*. **30**, 132, (1996).
- 11) P. Viktorovitch, M. Gendry, S. K. Krawczyk, F. Krafft, P. Abraham, A. Bekkaoui and Y. Monteil, *Appl. Phys. Lett.* **58** (1991) 2387.
- 12) D. A. Harrison, R. Ares, S. P. Watkins, M. L. W. Thewalt, C. R. Bolognesi, D. J. Becket and A. J. SpringThorpe, *Appl. Phys. Lett.* **70**, 3275, (1997).
- 13) T. Hara, H. Suzuki and A. Suga, *J. Appl. Phys.* **62**, 4109, (1987).
- 14) J. W. Orton and P. Blood, *The Electrical Characterization of Semiconductor Measurement of Minority Carrier Properties*, ( Academic Press Inc., San Diego, 1990).
- 15) G. Wang, G. Y. Zhao, T. Soga, T. Jimbo and M. Umeno, *Jpn. J. Appl. Phys.* **37**, L1280, (1998).
- 16) J. Chevallier, W. C. Dautremont-Smith, C. W. Tu and S. J. Pearton, *Appl. Phys. Lett.* **49**,

406, (1985).

17) R. H. Parekh and A. M. Barnett, *IEEE Trans. Electron Devices*, **31**, 689, (1984).

## **Chapter 6 Hydrogenation of GaAs-on-Si Schottky diodes by H<sub>2</sub>+PH<sub>3</sub> plasma exposure**

### **6. 1 Introduction**

Hetero-epitaxy of GaAs on Si substrate is very promising for optoelectronic integration technology<sup>1, 2</sup>. In the future, it is expected to combine the superior properties of GaAs-based photonic devices with the sophisticated technology of silicon on one chip. However, as described in previous chapters, for GaAs grown on Si substrate there exists a lattice mismatch of around 4.1% and thermal expansion coefficient mismatch of around 60%. As a result, high density of dislocation ( $\sim 10^6 \text{ cm}^{-2}$ ) exists in the GaAs epilayer, which restricts the widespread application of this hetero-epitaxial technology<sup>3</sup>. It is well known that defects act as generation-recombination centers. For the GaAs Schottky diodes on Si, its performance is degraded by the presence of high reverse bias voltage leakage currents and premature breakdown of the diodes, whose origins are clearly related to the high defects, such as threading dislocation density in the material<sup>4</sup>. To improve the characteristics of the GaAs Schottky diodes on Si, several attempts have been made, such as, growth of low temperature nucleation layers and strained layer superlattice as buffer layers, thermal cycle growth, etc<sup>5</sup>. But for current epitaxial growth technologies, the generation of defects in GaAs epilayers on Si can not be avoided to the full extent and, therefore, passivation of the activity of these defects is very essential. As described in chapter 2, it has been shown that the H incorporation can effectively passivate the electrical activity of most shallow and deep defect states in GaAs on Si<sup>6</sup>. There have been some reports on the investigation of the hydrogen (H) plasma passivation effects on the GaAs Schottky diodes on Si. An increase in the reverse current characteristics of GaAs Schottky diodes on Si have been realized by H plasma exposure<sup>7</sup>. This can be attributed to the passivation by hydrogen of dangling or defective bonds associated with



dislocations which contribute to excess leakage current in diode structures. But exposure to H plasma apparently introduces defects which become visible under reverse-biased conditions, and limits the practical usefulness of the H plasma passivation technique. Reduction and recovery of the H-plasma-induced damage without negating the beneficial effects of H incorporation is required<sup>8)</sup>. On the other hand, phosphidization of GaAs surface by phosphine ( $\text{PH}_3$ ) plasma exposure has also been extensively investigated. It has been found that phosphorus atoms can effectively suppress the generation of plasma-induced damages and passivate defects on the surface of GaAs<sup>9)</sup>. Some improvement of the electrical properties of GaAs Schottky diodes grown on GaAs substrates, and a change in the position of the Fermi level at the surface have been reported by  $\text{PH}_3$  plasma passivation<sup>10)</sup>.

In this chapter, we present for the first time the dual passivation effects on GaAs Schottky diodes grown on Si substrate by  $\text{PH}_3$  ( $\text{PH}_3/\text{H}_2=10\%$ ) plasma passivation. Through one  $\text{PH}_3$  plasma exposure process, the surface phosphidization and defect hydrogenation effect on GaAs on Si can be simultaneously realized. The passivation effects have been examined by studying the electrical behaviors and by deep level transient spectroscopy (DLTS) of Au-GaAs Schottky diodes on Si substrate grown by metalorganic chemical vapor deposition (MOCVD). The organization of this chapter is as follows: In section 6. 2, experimental procedure are described. The properties of GaAs schottky diodes and plasma passivation effects are characterized in chapter 6. 3. Finally, this chapter is summarized in section 4. 4.

## **6. 2 Experimental procedure**

The GaAs epilayers on Si have been grown by atmospheric pressure metal-organic chemical vapor deposition (MOCVD) using two-step growth technique. The source materials for Ga and As are trimethylgallium (TMG) and  $\text{AsH}_3$ , respectively. Si substrate with an orientation of (001), tilted  $2^\circ$  toward [110], was used. The substrate was etched in aqueous solution of HF, and thermally

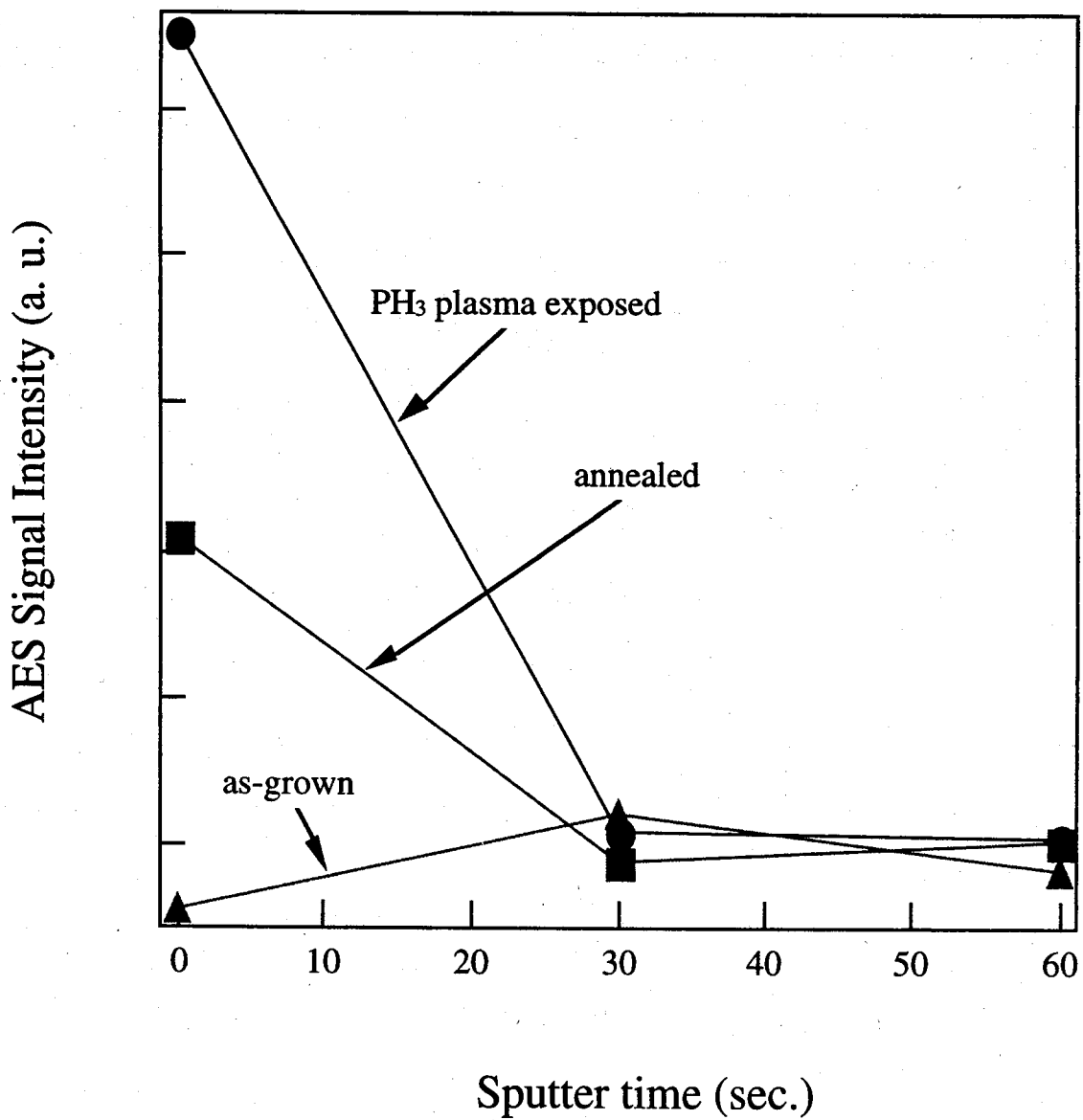


Fig. 6. 1 Auger signals of P atoms as a function of sputter time for the GaAs on Si substrates before, after PH<sub>3</sub> plasma exposure, and after annealing the PH<sub>3</sub> plasma exposed sample at 450°C for 10 min. in H<sub>2</sub> ambient.

cleaned at 1000°C for 10 min., followed by the growth of a thin GaAs buffer layer at 400°C. Then a 3 μm thick GaAs top layer was grown at 750°C. All the unintentionally doped GaAs layers are n-type ( $\sim 10^{17} \text{ cm}^{-2}$ ) due to the Si auto-doping during the growth process. After epitaxial growth, the passivation is carried out in H<sub>2</sub> and PH<sub>3</sub> (PH<sub>3</sub>/H<sub>2</sub>=10%) ambient at a reduced pressure (0.1 Torr). Typical plasma exposure conditions are 90 min at 250°C. In order to investigate the recovery of passivated donor states and the stability of passivated deep levels, a post-passivation annealing for some of the passivated samples was carried out in H<sub>2</sub> ambient at 450°C for 10 min. Auger electron spectroscopy (AES) was used to investigate the PH<sub>3</sub> plasma passivated GaAs surface. Then AuSb/Au ohmic contacts were formed by vacuum evaporation on the back side of the Si substrate, and annealed at 380°C for 30 sec. in a N<sub>2</sub> ambient. Finally, circular Gold Schottky contacts of 0.4 mm diameter were made on GaAs surface. Forward and reverse current-voltage (I-V) and capacitance-voltage (C-V) characteristics of Au-GaAs Schottky diodes on Si were measured at room temperature in dark. The capacitance (C) was measured at 100 kHz. DLTS measurements were carried out using an automated (HORIBA DA 1500) system at temperatures ranging from 100 K to 400 K.

### 6. 3 Characterization of the GaAs Schottky diodes on Si

Figure 6. 1 shows the Auger signals of P atoms as a function of sputter time for the GaAs on Si layers. After PH<sub>3</sub> plasma exposure, a strong phosphorus signal is observed on the surface of GaAs on Si, and the P atoms are still partly remained even after the annealing at 450°C for 10 min in H<sub>2</sub> ambient. However, after removing about 50 Å of the material, which corresponds to 30 sec. sputtering time, the AES signals intensity decrease down to its reference value. This means that PH<sub>3</sub> plasma exposure only induces a thin superficial P-related layer. That is to say, phosphidization modifies only the GaAs surface or the region located very close to the surface. On the other hand, the hydrogen atoms is incorporated to GaAs layer deeper than 2 μm<sup>8)</sup>.

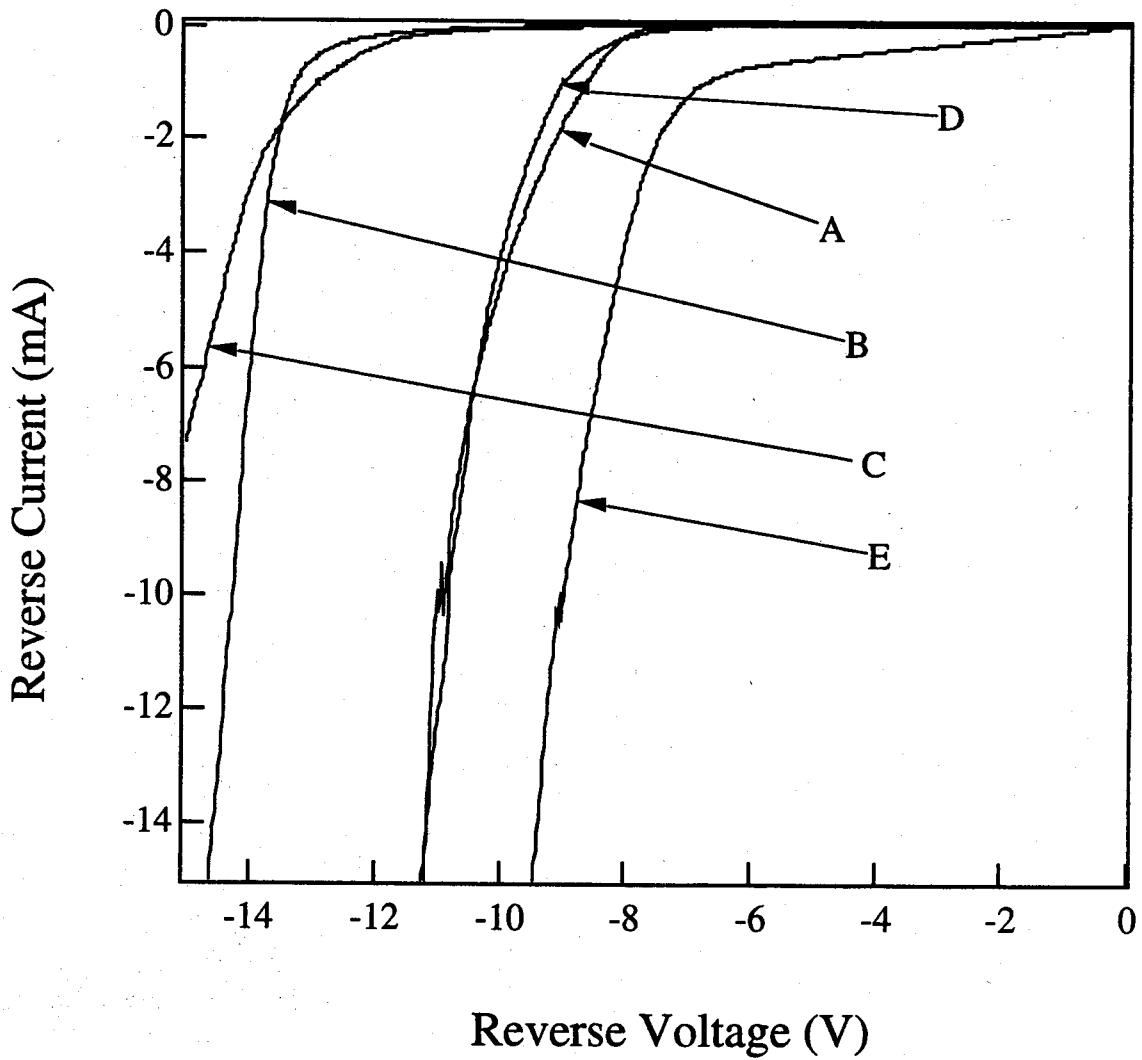


Fig. 6. 2 Reverse I-V characteristics of Au-GaAs Schottky diodes on Si substrates measured in dark at room temperature. The breakdown voltage is defined to be the reverse voltage at 1 mA. ( A: As-grown; B:  $\text{PH}_3$  plasma exposed; C:  $\text{H}_2$  plasma exposed; D:  $\text{PH}_3$  plasma exposed then annealed; E:  $\text{H}_2$  plasma exposed then annealed diodes).

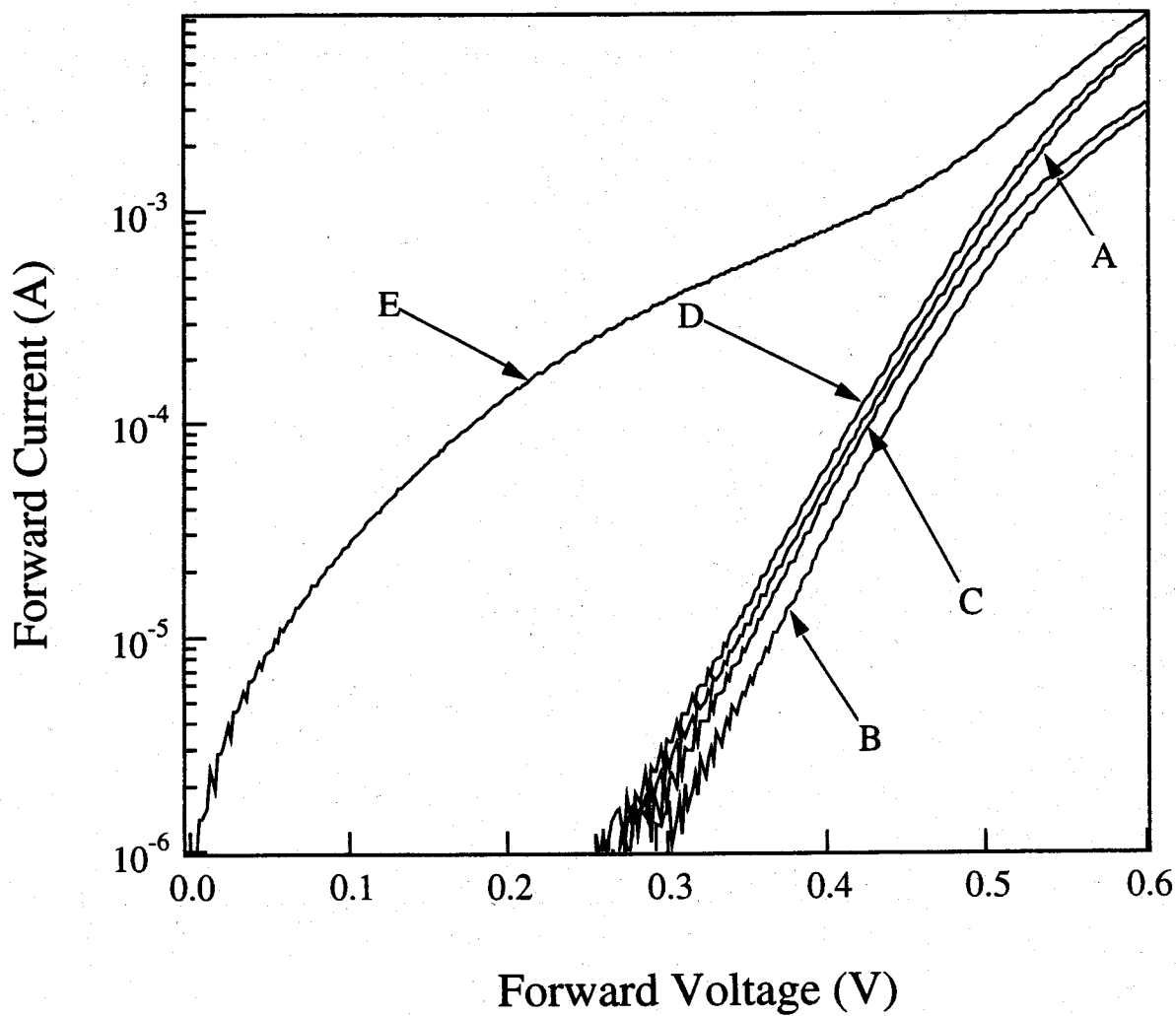


Fig. 6. 3 Forward I-V characteristics of Au-GaAs Schottky diodes on Si substrates measured in dark at room temperature. ( A: As-grown; B:  $PH_3$  plasma exposed; C:  $H_2$  plasma exposed; D:  $PH_3$  plasma exposed then annealed; E:  $H_2$  plasma exposed then annealed diodes).

Figure 6. 2 and 6. 3 show reverse and forward current-voltage (I-V) characteristics of Au-GaAs Schottky diodes on Si before and after PH<sub>3</sub> plasma exposure. For comparison, the I-V behavior of the H<sub>2</sub> plasma exposed Au-GaAs Schottky diodes on Si is also shown. It is clearly seen that both the PH<sub>3</sub> and H<sub>2</sub> plasma exposure induce a substantial increase in the reverse breakdown voltage ( $V_{br}$ ), which is the voltage at which the reverse leakage current is 1 mA. This improvement in the breakdown voltage in the plasma exposed diodes can be attributed to the passivation by H incorporation of the dislocation-related deep defects which increase the excess leakage current and cause the premature breakdown of the GaAs Schottky diodes on Si. But as shown in Fig. 6. 2, two differences are clearly seen between the reverse current characteristics of H<sub>2</sub> and PH<sub>3</sub> plasma exposed diodes; 1) H<sub>2</sub> plasma exposed GaAs Schottky diodes on Si show a "soft" breakdown, suggesting induction of more damaged surface[11]. 2) H<sub>2</sub> plasma exposed diodes have poor thermal stability. After annealing at 450°C for 10 min. to remove the the passivation effects of H atoms, the H<sub>2</sub> plasma exposed diodes become very leaky, but the PH<sub>3</sub> plasma exposed diodes still show a lightly good reverse I-V characteristics compared to that of the untreated diodes. This degradation of the H<sub>2</sub> plasma exposed GaAs Schottky on Si can be attributed to the plasma-induced damages. It is well known that atomic H will react with arsenic (As) and usually form an As deficient damaged GaAs surface by H<sub>2</sub> plasma exposure<sup>4)</sup>. For the as-passivated diodes, the plasma-induced defects are passivated by H atoms to some extent, but the 450°C-annealing removes the passivation effects of H and reactivates the plasma-induced damages. For the PH<sub>3</sub> plasma exposed diodes, via an As/P exchange mechanism, a very thin superficial layer of GaP is formed on the GaAs surface. P atoms are very effective in passivating defects on the surface of GaAs and suppress the generation of As-related plasma-induced defects. As shown in Fig. 6. 3, the forward I-V characteristics of the H<sub>2</sub> and PH<sub>3</sub> plasma exposed GaAs Schottky diodes on Si show little change except some decrease in the average ideality factors (n), which are summarized in Table 6. 1. This can be attributed to the fact that the forward current of GaAs Schottky diodes on Si is determined largely by thermionic emission. The annealing effects on the forward I-V

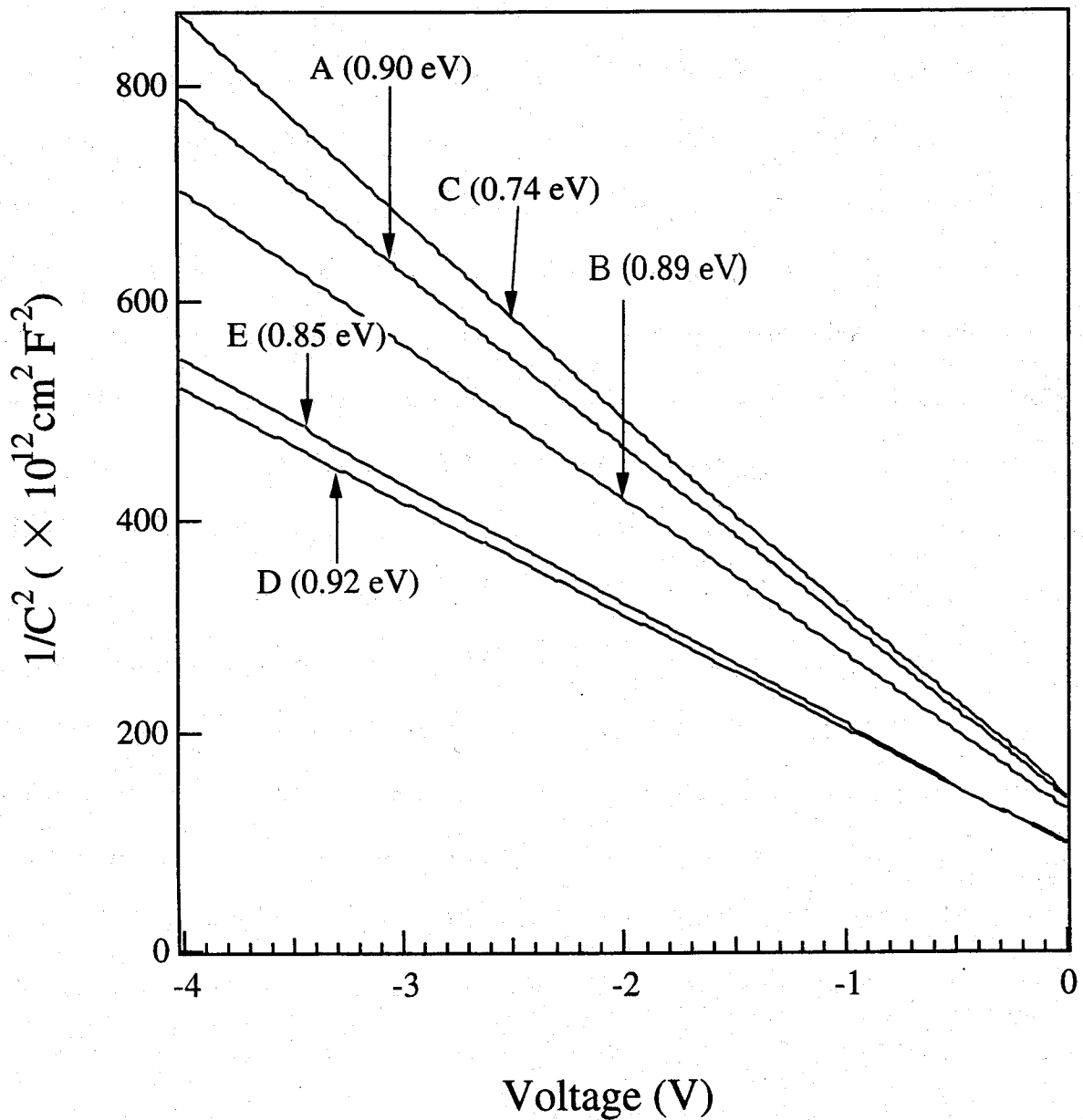


Fig. 6. 4 C-V characteristics of Au-GaAs Schottky diodes on Si substrates measured at room temperature for (A: As-grown; B: PH<sub>3</sub> plasma exposed; C: H<sub>2</sub> plasma exposed; D: PH<sub>3</sub> plasma exposed then annealed; E: H<sub>2</sub> plasma exposed then annealed diodes).

characteristics of plasma passivated diodes are very similar to that obtained from the reverse characteristics. The increased series resistance of the plasma exposed diodes can be attributed to the passivation by H of shallow dopants (Si) and reduced electron density.

Figure 6. 4 shows the C-V properties of the GaAs/Si schottky diodes before and after plasma passivation. The barrier height ( $\phi_{bn}$ ) of the GaAs Schottky diodes on Si was obtained from the intercept of the horizontal axis in the plots of  $C^{-2}$  vs.  $V$ , which is also shown in Table 6. 1. Comparing with the as-grown sample, it is clearly seen from Table I that  $\phi_{bn}$  is considerably reduced in both the  $H_2$  and  $PH_3$  plasma exposed diodes from 0.90 to 0.74 and 0.89 eV, respectively. As the As vacancies have a deep donor-like character<sup>12)</sup>, the decrease of the barrier height for this n-type GaAs on Si by plasma exposure can be related to the presence of plasma-induced donor like damage centers in the surface region<sup>13)</sup>. These effects are analogous to the influences of introducing defects by mechanically polishing the substrate before deposition of the metal contact<sup>14)</sup>. After annealing treatment,  $\phi_{bn}$  of  $H_2$  plasma exposed diodes was increased to 0.85 eV, but still small compared to that of the as-grown diode (0.9 eV). It means that thermal annealing at 450°C can not recovery the plasma induced damages on surface completely. In contrast, the annealing treatment increases  $\phi_{bn}$  of  $PH_3$  plasma exposed diodes to 0.92 eV. This increase in  $\phi_{bn}$  can only be attributed to the passivation effects of GaAs surface by P atoms incorporation, that reduce the surface state density.

The DLTS spectra obtained from all GaAs Schottky diodes on Si substrate are shown in Fig. 6. 5, except for the  $H_2$  plasma exposed then annealed diodes which is too leaky to measure. From the DLTS spectrum obtained from as-grown sample, three main electron traps EL2 (0.73 eV), ED1 (0.44 eV) and EL6 (0.32 eV) can be clearly seen. The EL6 deep level is very similarly to the T3 level described by K. Sakai et al., which may be due to lattice defect or donor-Ga-vacancy complex<sup>15)</sup>. The ED1 level is report by our group, which can be attributed to Si-dislocation complex which has a distributed energy centered at around 0.44 eV<sup>16)</sup>. It is readily seen that  $PH_3$  plasma exposure effectively reduces the concentration of all deep level. Most of all, the annealing of the



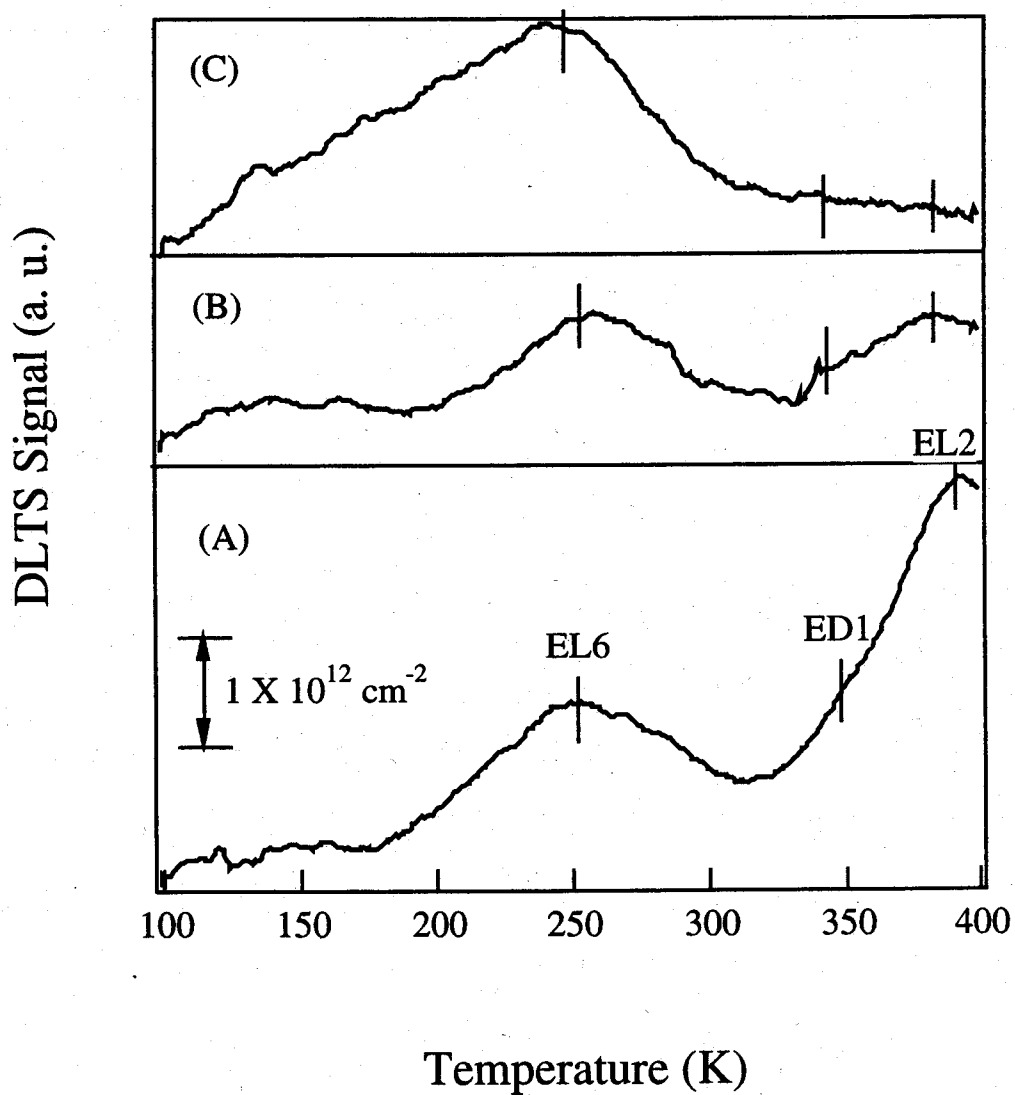


Fig. 6. 5 DLTS spectra of electron traps in unintentionally doped GaAs on Si substrate. The rate window is  $46.52 \text{ s}^{-1}$ . The trap concentration scale is indicated. ( A: As-grown; B:  $\text{PH}_3$  plasma exposed; C:  $\text{PH}_3$  plasma exposed then annealed diodes)

Table 6. 1  
 Average ideality factor  $n$ , Schottky barrier height  $\phi_{bn}$  and reverse breakdown voltage  $V_{br}$  in Au-GaAs Schottky diodes on Si substrate before and after plasma exposure.

Sample description	$n$	$V_{br}$ (V)	$q\phi_{bn}$ (eV)
as-grown	1.30	8.6	0.90
H <sub>2</sub> plasma exposed	1.27	12.9	0.74
H <sub>2</sub> plasma exposed then annealed	X	6.7	0.85
PH <sub>3</sub> /H <sub>2</sub> plasma exposed	1.21	13.3	0.89
PH <sub>3</sub> /H <sub>2</sub> plasma exposed then annealed	1.37	9.0	0.92

$\text{PH}_3$  plasma exposed GaAs on Si further reduces the concentration of EL2 centers, which are related to an isolated  $\text{As}_{\text{Ga}}$  or  $\text{As}_{\text{Ga}}$ -related complex. But compared to our previous results of the DLTS measurement on  $\text{H}_2$  plasma passivated GaAs on  $\text{Si}^{(8)}$ , post-plasma annealing treatment can not suppress the EL2 centers. This passivation effects can be attributed to the P atoms incorporation in the surface region of GaAs, which substitute the As-related defects. This gives a direct proof that both the phosphidization and hydrogenation effect on GaAs on Si are realized during one  $\text{PH}_3$ -added  $\text{H}_2$  plasma exposure process.

#### 6. 4 Conclusion

Both pure  $\text{H}_2$  and  $\text{PH}_3$ -added  $\text{H}_2$  passivation effects on GaAs Schottky diodes grown on Si substrates are investigated. It is found that the  $\text{PH}_3$  plasma passivation has a merit to realize the phosphidization and hydrogenation effect on GaAs on Si simultaneously by the P and H atoms incorporation. In addition, the  $\text{PH}_3$  plasma exposed GaAs Schottky diodes on Si have an excellent thermal stability compared to that of the  $\text{H}_2$  plasma exposed diodes. This gives a chance to utilize the plasma passivation technique in practical GaAs on Si device fabrication process.

## References:

- 1) T. Soga, T. Kato, M. Yang, T. Jimbo and M. Umeno, *J. Appl. Phys.* 78 (1995) 4196.
- 2) T. Egawa, H. Tada, Y. Kobayashi, T. Soga, T. Jimbo and M. Umeno, *Appl. Phys. Lett.* 57 (1990) 1179.
- 3) S. F. Fang, K. Adomi, S. Iyer, H. Morkoc, H. Zabel, C. Choi and N. Otsuka, *J. Appl. Phys.* 68 (1990) R31.
- 4) N. Chand, R. Fischer, A. M. Sergent, D. V. Lang, S. J. Pearton and A. Y. Cho, *Appl. Phys. Lett.* 51 (1987) 1013.
- 5) T. Egawa, S. Nozaki, N. Noto, T. Soga, T. Jimbo and N. Umeno, *J. Appl. Phys.* 67 (1990) 6908.
- 6) J. M. Zavada, S. J. Pearton, R. G. Wilson, C. S. Wu, Michael Stavola, F. Ren, J. Lopata, W. C. D-Smith and S. W. Novak, *J. Appl. Phys.* 65 (1989) 347.
- 7) S. J. Pearton, C. S. Wu, Michael Stavola, F. Ren, J. Lopata, W. C. Dautremont-Smith, S. M. Vernon and V. E. Haven, *Appl. Phys. Lett.* 51 (1987) 496.
- 8) G. Wang, G. Y. Zhao, T. Soga, T. Jimbo and M. Umeno: *Jpn. J. Appl. Phys.* 37 (1998) L1280.
- 9) T. Sugino, T. Yamada, K. Matsuda and J. Shirafuji, *Jpn. J. Appl. Phys.* 29 (1990) L1575.
- 10) T. Sugino, T. Yamada, K. Matsuda and J. Shirafuji, *Appl. Surf. Sci.* 56-58 (1992) 311.
- 11) E. H. Rhoderick, *Metal-semiconductor conducts* (Clarendon Press, Oxford London, 1978).
- 12) Y. X. Wang and P. H. Holloway, *J. Vac. Sci. Technol. B2* (1984) 613.
- 13) D. A. Vandenbroucke, R. L. V. Meirhaeghe, W. H. Laflere and F. Cardon, *Semicon. Sci. Technol.* 2 (1987) 293.
- 14) L. M. O. Vandenberghe, R. I. V. Meirhaeghe, W. H. Laflere and F. Cardon, *Solid-State Electron.* 29 (1986) 1109.
- 15) K. Sakai and T. Ikoma, *Appl. Phys.* 5 (1974) 165.
- 16) T. Soga, S. Sakai, M. Umeno and S. Hattori, *Jpn. J. Appl. Phys.* 25 (1986) 1510.

## Chapter 7 Summary

The practical importance of heteroepitaxy of GaAs-related compound semiconductor on Si substrate has long been recognized for its potential in optoelectronic integration technology. Extensive research has been pursued over the recent years, however, the dislocation densities of GaAs heteroepitaxial films on Si grown by any of the conventional methods such as the most common two-step growth technique, thermal anneal treatment, and use of strained layer superlattice are still largely over the order of  $10^6 \text{ cm}^{-2}$ . Since the generation of dislocations in GaAs epilayers on Si can not be avoided completely, an alternative approach is to passivate the electrical activity of these residual dislocations, rather than to reduce the dislocations density. The objective of this work is to establish a hydrogen plasma passivation method for passivation of the electrical activity of the defects related nonradiative recombination centers in GaAs on Si.

In this dissertation, the hydrogen plasma passivation effects on the GaAs-related compound semiconductors on Si grown by metal-organic chemical vapor deposition (MOCVD) were studied in details. The improvement of the properties of GaAs solar cells on Si were also demonstrated by hydrogen plasma passivation. In addition, in order to reduce the plasma-induced damages, a novel hydrogen plasma passivation method was developed by adding phosphine ( $\text{PH}_3$ ) into the hydrogen ( $\text{H}_2$ ) as a gas source during the RF plasma exposure process. It was found that the surface phosphidization and defect hydrogenation effects of GaAs solar cells on Si can be obtained simultaneously in this plasma exposure process. As a result, the properties of GaAs solar cells and Schottky diodes on Si were further improved.

In chapter 1, the purpose of this study, the present status of GaAs-related compound semiconductors on Si substrates were summarized, and the fundamental description of hydrogen plasma passivation was given. Scope of this dissertation was also presented.

In chapter 2, the effects of plasma hydrogenation on the optical and electrical properties of GaAs

on Si epitaxial layers is present, which are characterized by capacitance-voltage (C-V), photoluminescence (PL), time-resolved photoluminescence (TRPL) and deep-level transient spectra (DLTS) methods. We have observed that the H<sub>2</sub> plasma exposure improves significantly the PL properties and the minority carrier lifetime. In addition, the deep level which is related to Si-dislocation complex is completely passivated, and the effect of the deep level passivation retains even after annealing at 450°C for 10 min in AsH<sub>3</sub>/H<sub>2</sub> ambient.

In this chapter, also presented the defects passivation effects of hydrogen plasma exposure on the vertical-cavity surface-emitting laser (VCSEL) structure consisting of Al<sub>0.3</sub>Ga<sub>0.7</sub>As/GaAs multiple quantum well (MQW) active layer grown on Si substrates by PL measurement. It was found that the H<sub>2</sub> plasma exposure significantly increased the spontaneous emission intensity and quantum efficiency. This enhancement was attributed to the H<sub>2</sub> plasma passivation effect on the defects-related nonradiative recombination centers in GaAs/AlGaAs MQW on Si, and increased the minority carrier lifetime.

In chapter 3, H<sub>2</sub> plasma passivation and annealing effects on photovoltaic properties of GaAs/Si solar cell are studied in detail. The minority carrier lifetime is increased due to the H atoms passivation effects on defect-related nonradiative recombination centers. As a result, compared with that of the cell before H<sub>2</sub> plasma passivation (16.6%), an efficient increase in short circuit current density ( $J_{sc}$ ) and open circuit voltage ( $V_{oc}$ ) were realized due to the passivation of nonradiative recombination centers in GaAs/Si solar cell, as a result, a highest conversion efficiencies of 18.3% was obtained only by H<sub>2</sub> plasma exposure. But the plasma-induced damages still restrict the practical application of H<sub>2</sub> plasma passivation technology on GaAs/Si solar cell. In order to further increase the conversion efficiency of the H passivated GaAs/Si solar cell, it needs to remove the negative effect of plasma-induced damages as best as possible.

In chapter 4, we have investigated the H<sub>2</sub> plasma passivation effect of MOCVD-grown Al<sub>0.13</sub>Ga<sub>0.87</sub>As on Si, using PL spectroscopy. It has been found that the 4.2 K PL intensity increases for the H plasma passivated sample with reduced carrier concentration, owing to the

passivation of nonradiative recombination centers. The passivation of residual impurity carbon in the  $\text{Al}_{0.13}\text{Ga}_{0.87}\text{As}$  on Si epilayer was directly confirmed based on the observations of the 4.2 K PL spectra of the samples. The passivation effect is found to persist even following annealing at  $450^\circ\text{C}$  for 10 min.

In chapter 5, the results of  $\text{PH}_3/\text{H}_2$  ( $\text{PH}_3/\text{H}_2 = 10\%$ ) plasma passivation studies performed on GaAs/Si solar cells are presented. Both the surface phosphidization and defect hydrogenation effects of GaAs/Si solar cells were realized simultaneously in a single plasma exposure process. Comparing with the  $\text{H}_2$  plasma passivated GaAs/Si solar cells, very high open-circuit voltage,  $V_{oc}$  (0.93 V), and fill factor,  $FF$  (80.9%), have been obtained for  $\text{PH}_3/\text{H}_2$  plasma passivated cell and which is attributed mainly to the drastic decrease in saturation current density ( $J_o$ ). The converse efficiency ( $E_{ff}$ ) of GaAs/Si solar cell increased from 15.9% for unpassivated one to 18.6% for  $\text{PH}_3/\text{H}_2$  plasma passivated one. In order to test the thermal stability, the  $\text{PH}_3/\text{H}_2$  passivated cell was annealed in  $\text{H}_2$  ambient at  $450^\circ\text{C}$ . The annealed cell (Cell D) still showed a very high  $E_{ff}$  (17.9%). The  $\text{PH}_3/\text{H}_2$  plasma passivated GaAs/Si solar cell show a superior thermal characteristics compared with the pure  $\text{H}_2$  plasma passivated cell. In addition,  $\text{PH}_3/\text{H}_2$  plasma exposure has been found to increase the minority carrier lifetime more effectively than  $\text{H}_2$  plasma exposure. This can only be attributed to the passivation of AlGaAs/GaAs interfacial defects-related nonradiative recombination centers by P atoms incorporation in the surface region and reduced the  $\text{H}_2$  plasma induced damages.

In chapter 6, both pure  $\text{H}_2$  and  $\text{PH}_3/\text{H}_2$  passivation effects on GaAs Schottky diodes grown on Si substrates were presented. It is found that the  $\text{PH}_3$  plasma passivation has a merit to realize the phosphidization and hydrogenation effects on GaAs on Si simultaneously by the P and H atoms incorporation. In addition, the  $\text{PH}_3/\text{H}_2$  plasma exposed GaAs Schottky diodes on Si have an excellent thermal stability compared with that of the  $\text{H}_2$  plasma exposed diodes. From the DLTS spectra obtained from the GaAs Schottky diodes on Si substrate, it was found that both the  $\text{H}_2$  and  $\text{PH}_3/\text{H}_2$  plasma exposure effectively reduces the concentration of most deep levels. Furthermore, the annealing of the  $\text{PH}_3/\text{H}_2$  plasma exposed GaAs on Si further reduces the concentration of EL2

centers, which are related to an isolated  $As_{Ga}$  or  $As_{Ga}$ -related complex. This passivation effects can be attributed to the P atoms incorporation in the surface region of GaAs , which substitute the As-related defects.

### Scope for the future work

The hydrogen plasma passivation effects of GaAs-related compound semiconductors on Si substrates and its applications to optical and electrical devices were studied. The incorporation of hydrogen atoms passivated the electrical activity of the shallow and deep levels in GaAs on Si epilayer, which significantly improved the optical and electrical properties. After hydrogen plasma passivation, the conversion efficiencies of GaAs solar cells on Si were increased. For the GaAs Schottky diodes on Si, the forward and reverse characteristics were significantly improved. For the  $Al_{0.3}Ga_{0.7}As/GaAs$  multiple quantum well (MQW) vertical-cavity surface-emitting laser (VCSEL) structures on Si, a significant increase of the spontaneous emission intensity and quantum efficiency were presented. These results creates renewed prospects for the application of GaAs on Si to practical devices by utilizing defects passivation techniques. But exposure to  $H_2$  plasma also induces damages to GaAs surface, such as depletion of arsenic, which removes the beneficial effects of the H incorporation. It is necessary to remove the plasma-induced damages. Some damage control processes such as adding  $PH_3$  into  $H_2$  as a gas source has reduced the As-related plasma-induced damages to some extent. In addition, the recovery of the crystal quality by post annealing the passivated GaAs on Si in  $AsH_3$  ambient at  $450^\circ C$  after  $H_2$  plasma exposure was applied. But some ion damages still occurred during the plasma exposure process, and still remained even after post-plasma passivation annealing.

In the present rf plasma passivation process, the sample was exposed to a hydrogen plasma produced by the use of rf glow discharges. The sample, therefore, is subjected to ion and electron bombardment, and hence, the surface will be damaged. To avoid surface damage, it is necessary to



use some alternative method for the injection of atomic hydrogen into GaAs related compound semiconductor without ion and electron bombardment. Thus, the sample surface will not be deteriorated during the process. For example, proceeding the hydrogenation process in a photo chemical vapor deposition system (photo-CVD) was reported as an excellent tool to inject atomic hydrogen into crystalline semiconductor without surface damage<sup>1)</sup>. For the rf plasma generator used in present study, it is required to further reduce the ion flux incident on the sample surface, such as using of SiN<sub>x</sub> as an encapsulant to protect the surface during the plasma exposure processes. In addition, using an electrical shield around the sample during plasma exposure seems an effective method to reduce the extent of plasma-induced damage significantly<sup>2)</sup>. In order to suppress the depletion of arsenic from the GaAs surface, adding AsH<sub>3</sub> into pure H<sub>2</sub> during plasma exposure is thought to reduce the generation of As-related defects. But an As-rich layer on GaAs surface that simultaneously increases the interface trap intensity, it is also required to optimize the amount of As on GaAs surface to lower the trap density. Post-plasma rapid thermal annealing (RTA) is another promising method to recover the crystal quality from the ion damages. But it is necessary that RTA not eliminate the effects of hydrogen incorporation, because RTA usually needs a higher temperature.

As we have seen when we go through this dissertation, the thermal stability of the hydrogen plasma passivation effects is not high enough to make hydrogenation useful in most application. Annealing at 400~450°C completely recover the activity of the passivated shallow states, and as the annealing temperature is raised above 650°C, the passivation effects of deep levels will almost be lost. It is necessary to develop some more thermally stable defects passivation methods. For example, the effects of lithium (Li) on the native defects in GaAs has been reported<sup>3)</sup>. It is expected the the diffusion of Li into GaAs on Si is a damage free and thermally stable defect passivation method. Furthermore, using deuterium (D) instead of hydrogen as a defect passivation element is also expected to induce a more thermal stability defect passivation effects in GaAs on Si, because it was found that the Si-D bonds in GaAs will be more difficulty to be dissociated than the Si-H

bonds<sup>4)</sup>.

The concentration of deep levels in GaAs on Si was significantly decreased after H<sub>2</sub> plasma passivation. But the mechanism of the hydrogen-defect reaction is still not understood completely. Especially, the hydrogen passivation of dislocations in GaAs on Si still need to be proved directly from theory and experiment. The interaction between hydrogen and dislocation will give more information of the incorporation of hydrogen atoms in heteroepitaxial layer, such as GaN on sapphire, etc. Indeed, a deeper understanding of the art and science of hydrogen in GaAs on Si is also necessary to improve the defect passivation techniques.

Undoubtedly, the only way to ensure the various defects do not degrade the electrical and optical properties of GaAs on Si is either to keep them out of the material to begin with, or to getter them to a known location away from the active regions of a device. But it has been strongly proved that, under the present crystal growth technique, the passivation of the defects is an alternative method to turn the GaAs-related compound semiconductors on Si into practical application.

**References:**

- 1) J. C. Fan, J. C. Wang and Y. F. Chen, *Appl. Phys. Lett.* **74** (1999) 1463.
- 2) N. DasGupta, R. Riemenschneider and H. L. Hartnagel, *J. Electrochem. Soc.* **140** (1993) 2038.
- 3) S. Arpiainen, K. Saarinen, J. T. Gudmundsson and H. P. Gislason, *Physica B.* **273-274** (1999) 701.
- 4) J. Chevallier, M. Babe, E. Constant, D. Loidant-Bernard and M. Constant, *Appl. Phys. Lett.* **75** (1999) 112.